3
Nonlocality in three qubit systems

3.1 INTRODUCTION

As discussed in the previous chapter, the violation of Bell inequality [Bell, 1964; Clauser *et al.*, 1969] by a pure bipartite state is a confirmation of genuine quantum correlations between two particles -such long-range correlations allow the use of entangled resources for many potential applications in quantum information and computation which are otherwise not possible using classical resources. However, there are sets of two-qubit mixed states which do not violate the Bell inequality for certain ranges of state parameters even though they are entangled for those particular ranges. Moreover, there exist separable states displaying efficient quantum correlations-as confirmed by discord- which are also not identified by the Bell inequality. The presence of noise further complicates the analysis by adding intricacies to the system. In order to address these issues, in the previous chapter, we proposed to modify the Bell inequality using cluster coefficients to analyze nonlocal correlations in two-qubit pure and mixed states in presence and absence of noise. We have shown that our operator identifies correlations in all pure two qubit states and classes of two-qubit mixed and separable states where the Bell inequality fails to detect quantum correlations. We further found that results obtained in the previous chapter are also consistent with quantum discord.

Increasing the number of qubits in a state further increases the complexity of the problem. For example, unlike two-qubit generalized pure states, three-qubit entangled states can be distinguished as two separate distinct inequivalent classes, namely the *GHZ* and the *W* class. Moreover, for two-qubit entangled systems, the Bell inequality was violated by all pure entangled states and there are sets of mixed states which do not violate the Bell inequality. On the other hand, for three-qubit systems, there exist states well within the sets of entangled pure states which do not violate Bell-type inequalities. For example, one of the Bell-type inequalities to characterize nonlocality in three-qubit systems is the Mermin inequality [Mermin, 1990b]. The Mermin inequality fails to distinguish between bipartite and genuine tripartite nonlocal correlations as the inequality is violated by bi-separable as well as genuinely entangled three qubit states. Moreover, within the set of three-qubit pure *GGHZ* states, the inequality also fails to characterize nonlocality in a large set of states, i.e., the Mermin inequality is violated by *GGHZ* states only for $\tau(|\psi_{GHZ}\rangle) \geq \frac{1}{2}$, where τ is known as three-tangle which is an entanglement measure for three qubit states [Coffman *et al.*, 2000]. There is another instance of the Mermin inequality where the inequality is satisfied by all states having $\tau < \frac{1}{4}$ [Chi *et al.*, 2010]. The issue of distinguishing between bipartite and tripartite nonlocality can be successfully addressed using the Svetlichny inequality [Svetlichny, 1987]. Unlike the Mermin inequality, the Svetlichny inequality confirms the presence of genuine three-qubit correlations and acts as a signature of genuine three-qubit nonlocality, but then fails to characterize nonlocal correlations in *GHZ* class of states with $\tau(|\psi_{GHZ}\rangle) \leq \frac{1}{2}$.

In general, there is no generic inequality to discuss and compare nonlocality in multi-qubit states. The situation becomes even more complex when we move from three-qubit to four and five qubit states, as we will discuss in the next chapter. Therefore, in this chapter, we readdress the question of analyzing nonlocal correlations in three-qubit pure and mixed states in presence of noise. We start our discussion by establishing an analytical relation between the maximum expectation value of our proposed operator with the three-qubit entanglement measure in the

GGHZ class and then compare the analytical results with the numerical optimization. For real experimental scenario, we further extend our discussion to characterize nonlocality in three qubit states in presence of noise with and without applications of weak measurement and its reversal operations. For the purpose of our analysis and comparison of results, we use several sets of pure three-qubit entangled states belonging to *GHZ* and *W* class of states. In order to analyze nonlocal correlations in these states, we propose two different operators based on cluster coefficients and existing Bell-type inequalities. Our results show that the violation of modified inequalities act as an imprint of genuine nonlocality between three qubits. Moreover, we further demonstrate that all three-qubit entangled pure states violate the modified inequalities for the complete range of three-qubit entanglement measure. Further, our operators also succeed to distinguish between bipartite and tripartite nonlocality efficiently.

The remainder of the chapter is arranged as follows: in Section 3.2, we discuss modifications to existing Bell-type inequalities based on cluster coefficients. We further provide a detailed discussion on the identification of nonlocality in three-qubit *GGHZ* states using proposed operators in Section 3.3. This section also discusses effects of noise and weak measurement operations on the nonlocality of *GGHZ* states. Next few sections investigate the nonlocality of other three-qubit pure entangled states, i.e., $|\Phi\rangle$, *MS*, *W*, W_n states, e.g., in Section 3.4, Section 3.5, Section 3.6 and Section 3.7 respectively. We then extend our analysis to three-qubit mixed states in Section 3.8. We finally consider depolarizing channel to identify nonlocal correlations of three qubit states in noisy environment using our operators in Section 3.9 and finally in Section 3.10, we conclude the chapter.

3.2 MODIFIED INEQUALITIES

In Chapter 2, we discussed nonlocal correlations in two-qubit pure and mixed states using the modified operator in the presence and absence of noise. Similar to the Bell-CHSH inequality, our results also suggest the existence of nonlocality in all pure two-qubit entangled states. For mixed states, we have shown that our operator identifies correlations in separable states as well as mixed entangled states where the Bell inequality fails to identify nonlocal correlations. The results obtained in the previous chapter are also consistent with discord which is a signature of the presence of nonlocal correlations in an underlying two-qubit state. Clearly, identifying quantum correlations in entangled or separable states paves a way for their use as efficient resources for quantum information and computation. On the similar lines with quantum discord for two-qubit systems, there are some discord-type measures for quantifying quantum correlations in three-qubit systems [Rulli and Sarandy, 2011; Chakrabarty *et al.*, 2011] as well. However, the analytical evaluation of these measures is challenging due to the requirements of optimization/minimization involved in respective definitions. Therefore, in this chapter, we extend our discussion regarding identification of nonlocal correlations to three-qubit systems. Our discussion in this chapter is concentrated on analyzing nonlocal correlations in pure three qubit states belonging to the GHZ and W classes considering noise to be an inevitable effect.

In order to identify nonlocal correlations in three-qubit systems, we use Ursell-Mayer type expansions of correlation coefficients [Fano, 1983; Huang, 1987; Watson, 1956; Osborn, 1977; Schlienz and Mahler, 1995; Kumar and Krishnan, 2009b] discussed in the previous chapter to further propose the three-qubit operator. For this, we express correlation coefficients for a three-qubit system as [Huang, 1987; Osborn, 1977; Schlienz and Mahler, 1995; Kumar and Krishnan, 2009b]

$$C_{ijk}^{123} = \langle \sigma_i^1 \sigma_j^2 \sigma_k^3 \rangle - \langle \sigma_i^1 \rangle \langle \sigma_j^2 \sigma_k^3 \rangle - \langle \sigma_j^2 \rangle \langle \sigma_i^1 \sigma_k^3 \rangle - \langle \sigma_k^3 \rangle \langle \sigma_i^1 \sigma_j^2 \rangle + 2 \langle \sigma_i^1 \rangle \langle \sigma_j^2 \rangle \langle \sigma_k^3 \rangle \tag{3.1}$$

where σ's are Pauli spin operators, $i, j, k = x, y, z$ and 1, 2, 3 represent qubit indices. In accordance with our analysis in the previous chapter, we modify the Mermin inequality [Mermin, 1990b; Chi

et al., 2010] using above expressions for three-qubit correlation coefficients such that

$$|M_{cum}| = |\langle ABC\rangle_{cum} - \langle AB'C'\rangle_{cum} - \langle A'BC'\rangle_{cum} - \langle A'B'C\rangle_{cum}| \tag{3.2}$$

where

$$\langle ABC\rangle_{cum} = \langle ABC\rangle - \langle A\rangle\langle BC\rangle - \langle B\rangle\langle AC\rangle - \langle C\rangle\langle AB\rangle + 2\langle A\rangle\langle B\rangle\langle C\rangle \tag{3.3}$$

and $\langle AB'C'\rangle_{cum}$, $\langle A'BC'\rangle_{cum}$, $\langle A'B'C\rangle_{cum}$ are defined in a similar fashion. Here $A = \vec{a}.\vec{\sigma}_1$ and $A' = \vec{a'}.\vec{\sigma}_1$ are measurements performed on the first subsystem. Similarly $B = \vec{b}.\vec{\sigma}_2$ and $B' = \vec{b'}.\vec{\sigma}_2$ are measurements performed on the second subsystem whereas $C = \vec{c}.\vec{\sigma}_3$ and $C' = \vec{c'}.\vec{\sigma}_3$ are measurements performed on the third subsystem. As defined earlier $\vec{\sigma}_i = \{\sigma_x, \sigma_y, \sigma_z\}$ (with $i = 1,2,3$) are spin projection operators, and $\vec{a}$, $\vec{b}$, $\vec{c}$, $\vec{a'}$, $\vec{b'}$, $\vec{c'}$ are unit vectors in $\mathbb{R}^3$, defined as

$$\begin{aligned}
\vec{a} &= (Sin\theta_a Cos\phi_a, Sin\theta_a Sin\phi_a, Cos\theta_a)\\
\vec{b} &= (Sin\theta_b Cos\phi_b, Sin\theta_b Sin\phi_b, Cos\theta_b)\\
\vec{c} &= (Sin\theta_c Cos\phi_c, Sin\theta_c Sin\phi_c, Cos\theta_c)
\end{aligned} \tag{3.4}$$

Likewise, $\vec{a'}$, $\vec{b'}$ and $\vec{c'}$ can be defined in a similar manner with a prime on angles.

For three-qubit entangled systems, the Svetlichny inequality distinctly distinguishes between bipartite and tripartite nonlocality and thus the inequality is of immense value for analyzing genuine tripartite nonlocal correlations. Although the violation of three-qubit Svetlichny inequality is considered as a signature for the existence of genuine three-qubit nonlocality, the inequality cannot identify nonlocal correlations in all three-qubit pure entangled states in the GHZ class. Therefore, in this chapter, we also consider the three-qubit Svetlichny inequality in addition to the Mermin inequality and modify the Svetlichny inequality in a similar manner as we have modified the Mermin inequality, to get

$$\begin{aligned}
|S_{cum}| =& |\langle ABC\rangle_{cum} + \langle AB'C\rangle_{cum} + \langle ABC'\rangle_{cum} - \langle AB'C'\rangle_{cum} + \langle A'BC\rangle_{cum}\\
&- \langle A'B'C\rangle_{cum} - \langle A'BC'\rangle_{cum} - \langle A'B'C'\rangle_{cum}|
\end{aligned} \tag{3.5}$$

where all the terms involved can be defined in a similar fashion as above. The upper bounds of operators in Eq. (3.2) and Eq. (3.5) consistent with local correlations in three qubit states are 0. The original Mermin inequality- describes nonlocal correlations between any two particles and a local correlation with the third one- is violated by bi-separable as well as genuinely entangled three qubit states. Moreover, as discussed above, for three-qubit generalized-GHZ states, the the original Mermin and Svetlichny inequalities are violated only for $\tau(|\psi_{GHZ}\rangle) \geq \frac{1}{4}$ and $\tau(|\psi_{GHZ}\rangle) \geq \frac{1}{2}$, respectively where the degree of violation increases with the increase in degree of entanglement. The maximum violation is obtained for the maximally entangled *GHZ* state, i.e., $|GHZ\rangle = \frac{1}{\sqrt{2}}(|000\rangle + |111\rangle)$. Evidently the states in GGHZ class which do not violate the Mermin and Svetlichny inequalities, for the given range of τ, are entangled and therefore possess nonlocal correlations. Interestingly, our results show that the modified operators in both cases can be considered as an imprint for the presence of genuine three-qubit nonlocal correlations, as the inequality is not violated by product or bi-separable states. Moreover, both operators also identify nonlocal correlations in set of three-qubit entangled states which fail to violate Mermin and Svetlichny inequality. In fact the modified operators are violated by all pure three-qubit entangled states belonging to the GHZ and W class of states.

Before proceeding to analyze the modified Mermin and Svetlichny inequality in detail, we first briefly review the structure and classes of different three-qubit systems. A pure three-qubit state comprising of qubits *A*, *B* and *C* can be represented by one of the following ways depending on properties of the joint state, i.e.

- $|\psi_{A-B-C}\rangle = |\psi_A\rangle \otimes |\psi_B\rangle \otimes |\psi_C\rangle$: are direct product states without any nonlocal correlations;
- $|\psi_{A-BC}\rangle = |\psi_A\rangle \otimes |\psi_{BC}\rangle$, $|\psi_{B-AC}\rangle = |\psi_B\rangle \otimes |\psi_{AC}\rangle$, and $|\psi_{C-AB}\rangle = |\psi_C\rangle \otimes |\psi_{BC}\rangle$: are bi-separable states containing only bipartite nonlocal correlations in one of the partitions; and
- $|\psi_{ABC}\rangle$: are three qubit states exhibiting genuine three-qubit nonlocal correlations.

Since the Mermin inequality is violated by $|\psi_{ABC}\rangle$ as well as $|\psi_{A-BC}\rangle$ or $|\psi_{B-AC}\rangle$ or $|\psi_{C-AB}\rangle$, it cannot account for genuine tripartite nonlocal correlations. Svetlichny inequality, on the other hand, succeeds in successfully establishing the distinction between a bipartite and a tripartite nonlocality. We therefore begin our discussion by analyzing our operators with respect to product and bi-separable states and then take our discussion forward for three-qubit genuinely entangled classes. In view of this, we first evaluate the expectation values of our modified operators for three-qubit direct product states, i.e. $|\psi_{A-B-C}\rangle$, and three-qubit bi-separable states, i.e. ($|\psi_{A-BC}\rangle$ or $|\psi_{B-AC}\rangle$ or $|\psi_{C-AB}\rangle$). In general, the direct product and one of the bi-separable states $|\psi_{A-B-C}\rangle$ and $|\psi_{A-BC}\rangle$ can be represented as

$$|\psi_{A-B-C}\rangle = \{Cos\theta_1 |0\rangle + e^{i\phi_1} Sin\theta_1 |1\rangle\}_A \otimes \{Cos\theta_2 |0\rangle + e^{i\phi_2} Sin\theta_2 |1\rangle\}_B \otimes \{Cos\theta_3 |0\rangle + e^{i\phi_3} Sin\theta_3 |1\rangle\}_C \tag{3.6}$$

and

$$|\psi_{AB-C}\rangle = \frac{1}{\sqrt{2}}\{Cos\theta_1(|00\rangle + |11\rangle) + e^{i\phi_1} Sin\theta_1(|01\rangle - |10\rangle)\}_{AB} \otimes \{Cos\theta_2 |0\rangle + e^{i\phi_2} Sin\theta_2 |1\rangle\}_C \tag{3.7}$$

respectively. Similarly, one can also represent other bi-separable states $|\psi_{B-AC}\rangle$ or $|\psi_{C-AB}\rangle$. The first term, from Eq. (3.2), representing the expectation value $\langle ABC\rangle_{cum}$ for direct product (Eq. (3.6)) and bi-separable (Eq. (3.7)) states are evaluated to be

$$\langle ABC\rangle_{cum} = \langle \psi_{A-B-C}| ABC_{cum} |\psi_{A-B-C}\rangle = 0 \tag{3.8}$$

and

$$\langle ABC\rangle_{cum} = \langle \psi_{A-BC}| ABC_{cum} |\psi_{A-BC}\rangle = 0 \tag{3.9}$$

In the same way, we further evaluate other terms in Eq. (3.2) and Eq. (3.5) and find all expectation values to be 0. Combining all expectation values in Eq. (3.2) and Eq. (3.5), we therefore obtain $|M_{cum}| = |S_{cum}| = 0$ for both product and bi-separable states. Hence, the maximum expectation value of modified operators for all three-qubit product and bi-separable states are 0. Therefore a violation of modified inequalities using our operator bears a natural confirmation of existence of genuine three-qubit nonlocal correlations between qubits. In other words, for $|M_{cum}| > 0$ or $|S_{cum}| > 0$, modified inequalities confirm the presence of genuine three-qubit nonlocality. Clearly, in both the cases, our operators distinguish between bipartite and genuine tripartite nonlocalities whereas the optimal expectation value of the original Mermin operator exceeds its classical bound for bi-separable as well as three-qubit entangled states. In the next sections, we continue our discussion of tripartite nonlocality using the proposed operators in three-qubit pure and mixed entangled states.

3.3 NONLOCALITY IN GGHZ STATES

We start our discussion by considering one of the most widely used class of pure three-qubit entangled states, i.e., the GHZ class where a generalized state of the three-qubit *GHZ* class can be expressed as

$$|\psi_{GHZ}\rangle = Cos\theta |000\rangle + e^{i\phi} Sin\theta |111\rangle \tag{3.10}$$

For $\theta = \frac{\pi}{4}$ and $\phi = 0$, above state is the maximally entangled three-qubit *GHZ* state. The usefulness of *GHZ* class of states as resources for several efficient applications in quantum information and computation have been ascertained in the literature [Karlsson and Bourennane, 1998; Hillery *et al.*, 1999; Gorbachev and Trubilko, 2000; D'Hondt and Panangaden, 2004; Yang *et al.*, 2009a; Zhang *et al.*, 2009; Banerjee and Pathak, 2012; Chang *et al.*, 2013]. Although $|\psi_{GHZ}\rangle$ states are entangled for the complete range of parameters, i.e. $0 < \theta \leq \frac{\pi}{4}$ and $0 \leq \phi \leq \pi$, Mermin and Svetlichny inequalities are not violated by set of *GHZ* states as discussed earlier. In this section, we therefore analyze the usefulness of our operator to show that the proposed inequality indeed captures nonlocality in all *GHZ* states, i.e. for the complete range of parameters θ and ϕ.

Analytical Solution: In this section, we emphasize on optimizing the expectation value of the modified Mermin operator using cluster coefficients in a similar manner as we discussed in the previous chapter for the modified Bell operator. In pursuance of optimizing the operator represented in Eq. (3.2), we start our discussion by evaluating the expectation value $\langle ABC\rangle_{cum}$, such that

$$\begin{aligned}\langle ABC\rangle_{cum} &= \langle \psi_{GGHZ}| (ABC)_{cum} |\psi_{GGHZ}\rangle \\ &= -Sin2\theta Sin4\theta Cos\theta_a Cos\theta_b Cos\theta_c + Sin2\theta Sin\theta_a Sin\theta_b Sin\theta_c \\ &\quad [Cos\phi\ Cos(\phi_a+\phi_b+\phi_c) + Sin\phi\ Sin(\phi_a+\phi_b+\phi_c)] \end{aligned} \tag{3.11}$$

We now optimize the expectation value $\langle ABC\rangle_{cum}$ with respect to $\phi_a+\phi_b+\phi_c$, using $p\,Sin\theta + q\,Cos\theta \leq \sqrt{p^2+q^2}$, and $Cos^2\phi + Sin^2\phi = 1$, to get

$$\langle ABC\rangle_{cum} \leq Sin2\theta [Sin\theta_a Sin\theta_b Sin\theta_c - Sin4\theta Cos\theta_a Cos\theta_b Cos\theta_c] \tag{3.12}$$

In a similar fashion, we also evaluate

$$\langle AB'C'\rangle_{cum} \leq Sin2\theta [Sin\theta_a Sin\theta'_b Sin\theta'_c - Sin4\theta Cos\theta_a Cos\theta'_b Cos\theta'_c] \tag{3.13}$$

$$\langle A'BC'\rangle_{cum} \leq Sin2\theta [Sin\theta'_a Sin\theta_b Sin\theta'_c - Sin4\theta Cos\theta'_a Cos\theta_b Cos\theta'_c] \tag{3.14}$$

$$\langle A'B'C\rangle_{cum} \leq Sin2\theta [Sin\theta'_a Sin\theta'_b Sin\theta_c - Sin4\theta Cos\theta'_a Cos\theta'_b Cos\theta_c] \tag{3.15}$$

Using expectation values of $\langle ABC\rangle_{cum}$, $\langle AB'C'\rangle_{cum}$, $\langle A'BC'\rangle_{cum}$, and $\langle A'B'C\rangle_{cum}$ from Equations (3.12), (3.13), (3.14) and (3.15) in Eq. (3.2), we obtain

$$\begin{aligned}|M_{cum}| \leq Sin2\theta \big[&Sin\theta_a\{Sin\theta_b Sin\theta_c + Sin\theta'_b Sin\theta'_c\} - Sin4\theta Cos\theta_a\{Cos\theta_b Cos\theta_c + Cos\theta'_b Cos\theta'_c\} \\ &+ Sin\theta'_a\{Sin\theta_b Sin\theta'_c + Sin\theta'_b Sin\theta_c\} - Sin4\theta Cos\theta'_a\{Cos\theta_b Cos\theta'_c + Cos\theta'_b Cos\theta_c\}\big] \end{aligned} \tag{3.16}$$

One can further maximize Eq. (3.16) with respect to θ_a and θ'_a, such that

$$\begin{aligned}|M_{cum}| \leq Sin2\theta \big[&\big[\{Sin\theta_b Sin\theta_c - Sin\theta'_b Sin\theta'_c\}^2 + Sin^2 4\theta\{Cos\theta_b Cos\theta_c - Cos\theta'_b Cos\theta'_c\}^2\big]^{1/2} \\ &+ \big[\{Sin\theta_b Sin\theta'_c + Sin\theta'_b Sin\theta_c\}^2 + Sin^2 4\theta\{Cos\theta_b Cos\theta'_c + Cos\theta'_b Cos\theta_c\}^2\big]^{1/2}\big] \end{aligned} \tag{3.17}$$

Using binomial expansion for simplification, we further express Eq. (3.17) as

$$\begin{aligned}|M_{cum}| &\leq Sin2\theta \big[Sin\theta_b Sin\theta_c + Sin\theta'_b Sin\theta'_c + Sin\theta_b Sin\theta'_c + Sin\theta'_b Sin\theta_c\big] \\ &\leq Sin2\theta \big[Sin\theta_b(Sin\theta_c + Sin\theta'_c) + Sin\theta'_b(Sin\theta_c + Sin\theta'_c)\big] \end{aligned} \tag{3.18}$$

We now optimize the above expression with respect to θ_b and θ'_b by considering $\theta_b = \theta'_b = \frac{\pi}{2}$, therefore the maximum expectation value of modified Mermin operator is given as

$$|M_{cum}| \leq 2Sin2\theta [Sin\theta_c + Sin\theta'_c] \tag{3.19}$$

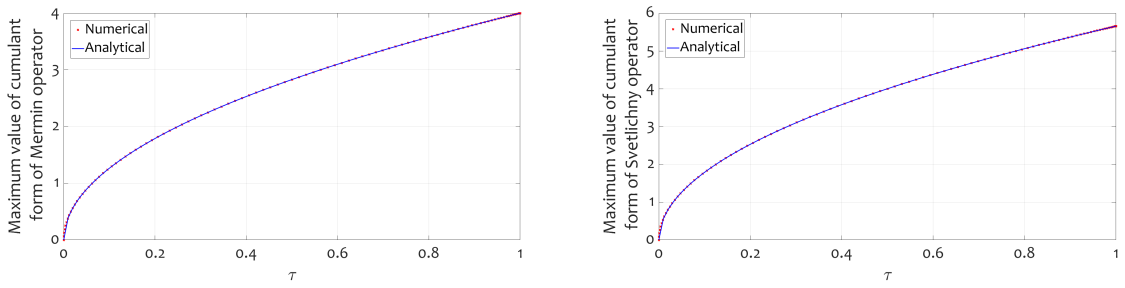

(a) (b)

Figure 3.1 : Comparison of analytical and numerical results for maximum expectation values of (a) $|M_{cum}|$, (b) $|S_{cum}|$ versus three-tangle (τ) for $GGHZ$ states

A further consideration of $\theta_c = \frac{\pi}{2}$ and $\theta_c' = \frac{\pi}{2}$, to optimize the expression for $|M_{cum}|$, results in

$$|M_{cum}| \leq 4Sin2\theta = 4\sqrt{\tau(|\psi_{GHZ}\rangle)} \tag{3.20}$$

The analytical results obtained here are in complete agreement with the numerical optimization as shown in Figure 3.1(a). Figure 3.1(a) clearly demonstrates that the inequality is violated for all $0 < \tau(|\psi_{GHZ}\rangle) \leq 1$ where $\tau(|\psi_{GHZ}\rangle) = Sin^2(2\theta))$ with the maximum value ($\tau = 1$) corresponding to the maximally entangled GHZ state. Similar to the case of a pure pure two-qubit entangled state, the degree of violation of GHZ states increases with the increase in degree of entanglement and thus the maximal violation is obtained for the maximally entangled GHZ state. Therefore, unlike the original Mermin operator, our proposed operator not only distinguishes between bipartite and tripartite nonlocality, but also identifies nonlocal correlations in all entangled generalized GHZ states. Similar to the modified Mermin operator, the modified Svetlichny operator given in Eq. (3.5) also confirms the presence of nonlocal correlations in all generalized GHZ states with analytical solution as $|S_{cum}| \leq 4\sqrt{2}Sin2\theta = 4\sqrt{2\tau(|\psi_{GHZ}\rangle)}$ which is further summarized in Figure 3.1(b). In this case also, in comparison to the original Svetlichny operator, our operator detects the existence of nonlocal correlations in all GHZ states; even when $\tau \leq \frac{1}{2}$. In other words, all pure three-qubit entangled states in GHZ class violate the $|M_{cum}|$ and $|S_{cum}|$ inequalities with degree of violation monotonically increasing for the range $0 < \tau \leq 1$. Figure 3.1(a) and Figure 3.1(b) show that the maximum violation using $|M_{cum}|$ is 4, whereas the maximum violation using $|S_{cum}|$ is $4\sqrt{2}$. In fact, the violation for $|S_{cum}|$ is always greater than $|M_{cum}|$ for all values of τ similar to the case of original inequalities in the range where both inequalities are violated. Nevertheless, both the inequalities succeed in successfully identifying genuine three-qubit nonlocality in all three-qubit pure entangled states belonging to the GHZ class. For executing the optimization of modified operators, $|M_{cum}|$ may have an edge over $|S_{cum}|$ due to the presence of less number of terms; this, however, by no means degrades the importance and utility of the Svetlichny operator in identifying and analyzing nonlocal correlations in entangled systems.

3.3.1 Nonlocality of GGHZ states in presence of noise and weak measurement operations

Similar to our discussion in the previous chapter and considering the imminent presence of noise, we now proceed to analyze effects of amplitude damping noise and weak measurement operations on the nonlocality of three-qubit $GGHZ$ states using our modified operators. For simplicity and mathematical convenience, we first consider that all three qubits of the $GGHZ$ state pass through amplitude damping channels of equal strengths. Using the operator sum representation and operational elements of an amplitude damping channel as represented in Eq. (1.44), the joint state of the three-qubit system after passing through amplitude damping

channels can be represented as

$$\rho^{AD}_{GGHZ} = \begin{bmatrix} C_\theta^2 + d^3 S_\theta^2 & 0 & 0 & 0 & 0 & 0 & 0 & \bar{d}^{3/2} e^{-\iota\phi} C_\theta S_\theta \\ 0 & \bar{d} d^2 S_\theta^2 & 0 & 0 & 0 & 0 & 0 & 0 \\ 0 & 0 & \bar{d} d^2 S_\theta^2 & 0 & 0 & 0 & 0 & 0 \\ 0 & 0 & 0 & \bar{d}^2 d S_\theta^2 & 0 & 0 & 0 & 0 \\ 0 & 0 & 0 & 0 & \bar{d} d^2 S_\theta^2 & 0 & 0 & 0 \\ 0 & 0 & 0 & 0 & 0 & \bar{d}^2 d S_\theta^2 & 0 & 0 \\ 0 & 0 & 0 & 0 & 0 & 0 & \bar{d}^2 d S_\theta^2 & 0 \\ \bar{d}^{3/2} e^{\iota\phi} C_\theta S_\theta & 0 & 0 & 0 & 0 & 0 & 0 & \bar{d}^3 S_\theta^2 \end{bmatrix} \tag{3.21}$$

here $C_\theta = Cos(\theta)$, $S_\theta = Sin(\theta)$ and $\bar{d} = 1 - d$. In order to characterize nonlocal correlations in *GGHZ* states in presence of noise, we optimize the expectation values of $|M_{cum}|$and $|S_{cum}|$ with respect to Eq. (3.21) in a similar manner as discussed in the ideal case. Figure 3.2 summarizes effects of amplitude damping channels on nonlocality of three-qubit general *GHZ* states using $|M_{cum}|$and $|S_{cum}|$ operators. The analytical results in this case are $|M_{cum}| \leq 4\bar{d}^{\frac{3}{2}}\sqrt{\tau(|\psi_{GHZ}\rangle)}$ and $|S_{cum}| \leq 4\bar{d}^{\frac{3}{2}}\sqrt{2\tau(|\psi_{GHZ}\rangle)}$. Expectedly, nonlocal correlations decrease with the increasing strength of

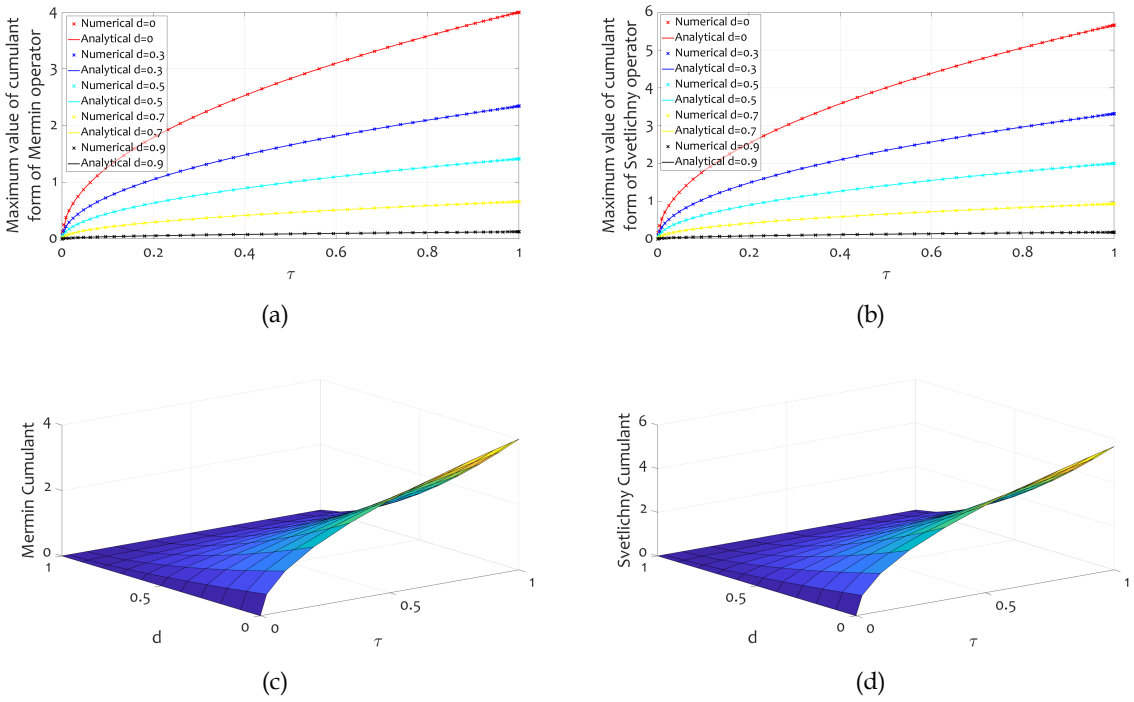

Figure 3.2 : Effects of amplitude damping noise on the nonlocality of *GGHZ* states using (a), (c) $|M_{cum}|$ and (b), (d) $|S_{cum}|$ operators

the amplitude damping noise and eventually cease to 0 for the maximum value of the decoherence parameter. Nevertheless, *GGHZ* states exhibit nonlocal correlations in both cases even when decoherence is very strong. At a particular value of the noise parameter, the optimal expectation value of $|S_{cum}|$ operator is always greater than the optimal expectation value of the $|M_{cum}|$ operator as found in the ideal case as well. Similar to the case of generalized two-qubit pure states discussed in the previous chapter, for *GGHZ* states, the maximum nonlocality coincides with maximum entanglement of the original input state. Therefore, in presence of amplitude damping channels, the maximally entangled *GHZ* state is more robust towards nonlocal correlations in comparison to other partially entangled states of the *GGHZ* class irrespective of the value of noise parameter. We further analyze nonlocal properties in *GGHZ* states using applications of weak measurement and its reversal operations to suppress the detrimental effects of amplitude damping channels.

For this, one needs to perform weak measurement operation on all qubits before they pass through amplitude damping channels, and weak measurement reversal operations once qubits pass through amplitude damping channels. The final state after passing through amplitude damping channels in presence of weak measurement operations is

$$\rho_{GGHZ}^{ADWM} = \frac{1}{A}\begin{bmatrix} C_\theta^2 + d^3\bar{w}^3 S_\theta^2 & 0 & 0 & 0 & 0 & 0 & 0 & e^{-\iota\phi} C_\theta S_\theta \\ 0 & d^2\bar{w}^2 S_\theta^2 & 0 & 0 & 0 & 0 & 0 & 0 \\ 0 & 0 & d^2\bar{w}^2 S_\theta^2 & 0 & 0 & 0 & 0 & 0 \\ 0 & 0 & 0 & d\bar{w} S_\theta^2 & 0 & 0 & 0 & 0 \\ 0 & 0 & 0 & 0 & d^2\bar{w}^2 S_\theta^2 & 0 & 0 & 0 \\ 0 & 0 & 0 & 0 & 0 & d\bar{w} S_\theta^2 & 0 & 0 \\ 0 & 0 & 0 & 0 & 0 & 0 & d\bar{w} S_\theta^2 & 0 \\ e^{\iota\phi} C_\theta S_\theta & 0 & 0 & 0 & 0 & 0 & 0 & S_\theta^2 \end{bmatrix} \tag{3.22}$$

here $\bar{w} = 1 - w$ and $A = Cos^2\theta + (1 + d\bar{w})^3 Sin^2\theta$. The correlations in the evolved mixed state can be further optimized using the optimal relation between the weak measurement parameter, the reversal operation parameter and the noise parameter as discussed in Chapter 1. We finally evaluate the maximum expectation values of $|M_{cum}|$and $|S_{cum}|$ operators using Eq. (3.22).

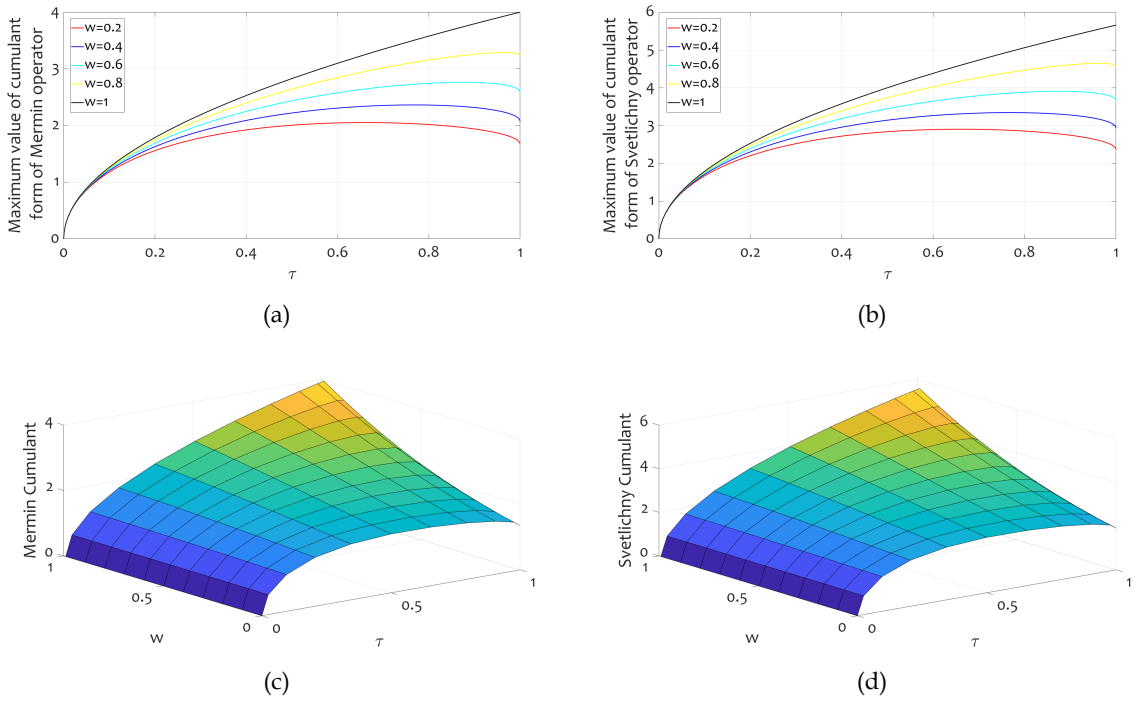

Figure 3.3 : Effects of weak measurement operations on the nonlocality of *GGHZ* states using (a), (c) $|M_{cum}|$ and (b), (d) $|S_{cum}|$ operators

Figure 3.3 represents a relation between the maximum expectation values of modified operators, degree of entanglement of original *GGHZ* states and different values of weak measurement operation for the value of decoherence parameter as 0.7. A comparison between Figure 3.2 and Figure 3.3 shows the usefulness of weak measurement technique for protecting nonlocal correlations in *GGHZ* states from decoherence. Interestingly, for lower values of the weak measurement parameter, set of partially entangled *GGHZ* states lead to maximum violation of $|M_{cum}|$ and $|S_{cum}|$ operators instead of the maximally entangled input state. This is completely in contrast to our discussion for *GGHZ* states in ideal case or in presence of noise without the applications of weak measurements. The behavior of nonlocal correlations in *GGHZ* states,

however, is similar to the one discussed in the previous chapter for two-qubit pure entangled states. As the value of weak measurement parameter increases, nonlocal correlations also increase and the set of *GGHZ* states showing nonlocality anomaly decreases. For higher values of weak measurement parameter, i.e.,$w = 1$, nonlocal correlations are restored to its original value with maximum nonlocality coinciding with the maximum entanglement of the original state. Therefore, even for higher values of decoherence parameter, one can revive nonlocal correlations to its original strength.

3.4 NONLOCALITY IN $|\Phi\rangle$ STATES

In this section, we analyze nonlocal properties of another important class of three-qubit pure entangled states, i.e., $|\Phi\rangle$ states, represented as

$$|\Phi\rangle = \frac{1}{\sqrt{2}}[Cos(\theta_\Phi)(|000\rangle + |011\rangle) + Sin(\theta_\Phi)(|110\rangle - |101\rangle)] \tag{3.23}$$

where $0 < \theta_\Phi \leq \frac{\pi}{4}$. The set of $|\Phi\rangle$ states belong to the three-qubit *GHZ* class found to be very useful in different quantum communication protocols in presence of noise [Faujdar and Kumar, 2019, 2021]. The degree of entanglement in $|\Phi\rangle$ states- as measured by three-tangle τ- is $\tau(|\Phi\rangle) = Sin^2(2\theta_\Phi)$. The set of states are entangled for all values of θ_Φ with $\theta_\Phi = \frac{\pi}{4}$ leading to a state locally equivalent to the maximally entangled GHZ state. In the ideal case, we optimize and evaluate the maximum expectation values of modified Mermin and Svetlichny operators with respect to all parameters involved as discussed in the case of *GGHZ* states. From Figure 3.4, our results indicate that all

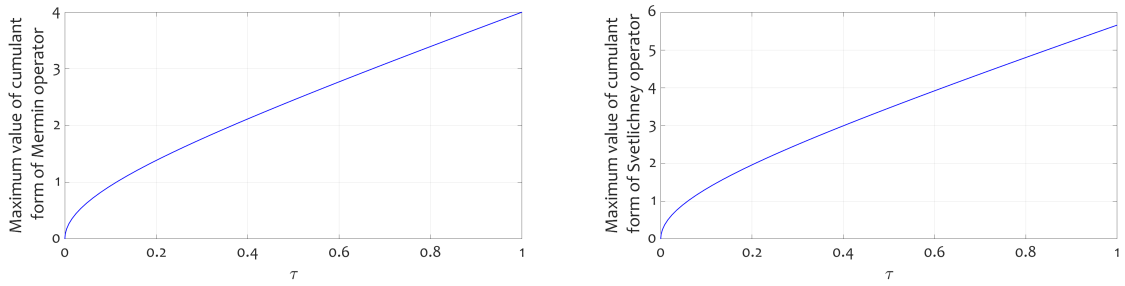

(a) (b)

Figure 3.4 : Maximum expectation values of (a) $|M_{cum}|$, (b) $|S_{cum}|$ operators versus three-tangle (τ) for $|\Phi\rangle$ states

$|\Phi\rangle$ states violate the proposed operators for the complete range of entanglement measure τ, and the violation monotonically increases from $\tau = 0$ to $\tau = 1$. The maximum violation belongs to the maximally entangled GHZ state (4 for $|M_{cum}|$ and $4\sqrt{2}$ $|S_{cum}|$), much like the case for *GGHZ* states. Although the degree of entanglement in *GGHZ* and $|\Phi\rangle$ states are same, nonlocal correlations in $|\Phi\rangle$ states are always less than the nonlocal correlations in *GGHZ* states. Evidently $|\Phi\rangle$ states show more violation towards the modified Svetlichny inequality as against the violation towards the modified Mermin inequality. We further discuss the properties and usefulness of these states in quantum information in a later chapter. Similar to original Mermin and Svetlichny operators, proposed operators also identify nonlocal correlations in all $|\Phi\rangle$ states.

3.4.1 Nonlocality of $|\Phi\rangle$ states in presence of noise and weak measurements

Similar to the case of *GGHZ* states, for simplicity and mathematical convenience, here also we consider all three qubits of $|\Phi\rangle$ states to pass through amplitude damping channels of equal strengths. Once the qubits pass through noisy channels, we characterize nonlocal correlations in

the evolved mixed state, i.e.

$$\rho_{\Phi}^{AD} = \frac{1}{2}\begin{bmatrix} (1+d^2)C_{\theta_\Phi}^2 + 2d^2S_\theta^2 & 0 & 0 & \bar{d}C_\theta^2 & 0 & -\frac{\bar{d}}{2}S_{2\theta} & \frac{\bar{d}}{2}S_{2\theta} & 0 \\ 0 & \bar{d}d & -\bar{d}dS_\theta^2 & 0 & \frac{\bar{d}d}{2}S_{2\theta} & 0 & 0 & 0 \\ 0 & -\bar{d}dS_\theta^2 & \bar{d}d & 0 & -\frac{\bar{d}d}{2}S_{2\theta} & 0 & 0 & 0 \\ \bar{d}C_\theta^2 & 0 & 0 & \bar{d}^2C_\theta^2 & 0 & -\frac{\bar{d}^2}{2}S_{2\theta} & \frac{\bar{d}^2}{2}S_{2\theta} & 0 \\ 0 & 0 & 0 & 0 & d^2\bar{w}^2S_\theta^2 & 0 & 0 & 0 \\ 0 & 0 & 0 & 0 & 0 & d\bar{w}S_\theta^2 & 0 & 0 \\ 0 & 0 & 0 & 0 & 0 & 0 & d\bar{w}S_\theta^2 & 0 \\ e^{\iota\phi}C_\theta S_\theta & 0 & 0 & 0 & 0 & 0 & 0 & S_\theta^2 \end{bmatrix} \tag{3.24}$$

using our proposed operators. Figure 3.5 demonstrates effects of amplitude damping noise

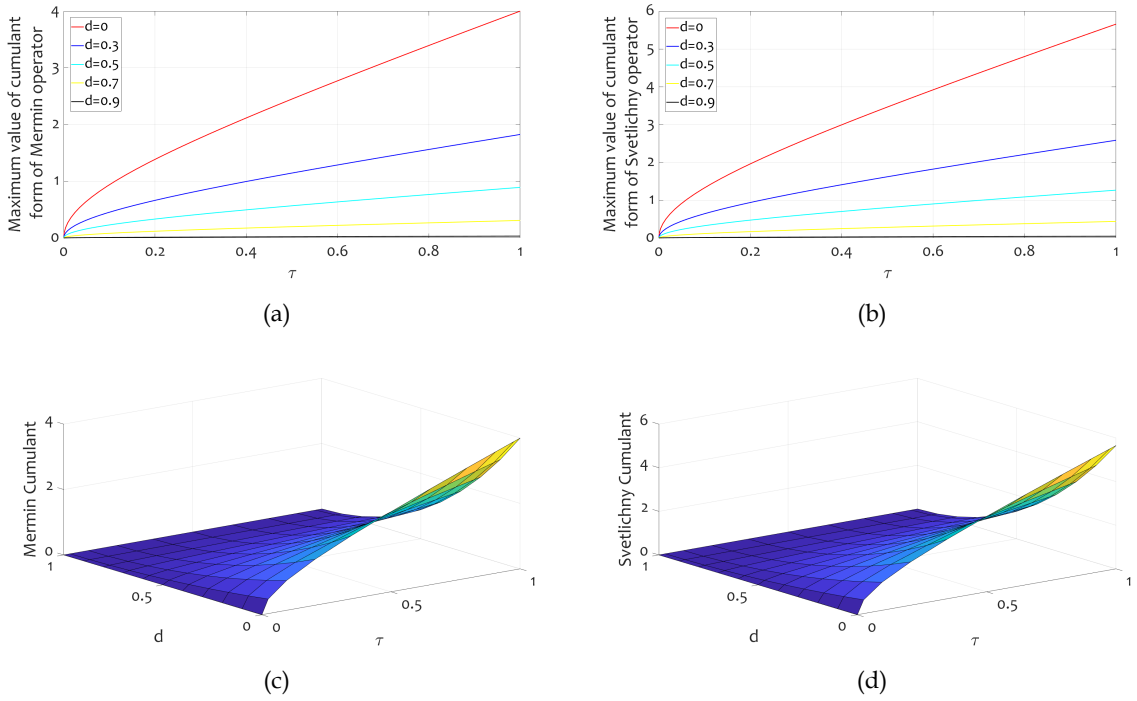

Figure 3.5 : Effects of amplitude damping noise on the nonlocality of $|\Phi\rangle$ states using (a), (c) $|M_{cum}|$ and (b), (d) $|S_{cum}|$ operators

on nonlocal correlations in $|\Phi\rangle$ states. The nonlocal correlations in $|\Phi\rangle$ states decrease rapidly with increasing strength of amplitude damping noise. Although $|\Phi\rangle$ states violate the modified inequalities, the degree of violation is very low for higher strengths of noise parameter. In fact, nonlocal correlations almost die for $d > 0.8$ in both the cases. Evidently *GGHZ* states are more robust to amplitude damping noise in comparison to $|\Phi\rangle$ states for the complete range of entanglement measure τ. This is reasonable as nonlocal correlations in *GGHZ* states are higher than nonlocal correlations in $|\Phi\rangle$ states in ideal case itself as verified from Figure 3.1 and Figure 3.4. Figure 3.5 further shows that $|\Phi\rangle$ states- much like *GGHZ* states- do not indicate any presence of nonlocality anomaly as increase in nonlocality monotonically coincides with increase in degree of entanglement of the original state. In order to analyze effects of weak measurement and its reversal operations on nonlocal correlations in presence of noise, we represent the evolved mixed

state under combined effects of weak measurements and amplitude damping channels as

$$\rho_{\Phi}^{ADWM} = \frac{1}{A}\begin{bmatrix} 1+3d^2\bar{w}^2+(1-d^2\bar{w}^2)C_{2\theta} & 0 & 0 & 2C_\theta^2 & 0 & -S_{2\theta} & S_{2\theta} & 0 \\ 0 & 2d\bar{w} & -2d\bar{w}S_\theta^2 & 0 & d\bar{w}S_{2\theta} & 0 & 0 & 0 \\ 0 & -2d\bar{w}S_\theta^2 & 2d\bar{w} & 0 & -d\bar{w}S_{2\theta} & 0 & 0 & 0 \\ 2C_\theta^2 & 0 & 0 & 2C_\theta^2 & 0 & -S_{2\theta} & S_{2\theta} & 0 \\ 0 & d\bar{w}S_{2\theta} & -d\bar{w}S_{2\theta} & 0 & 4d\bar{w}S_\theta^2 & 0 & 0 & 0 \\ -S_{2\theta} & 0 & 0 & -S_{2\theta} & 0 & 2S_\theta^2 & -2S_\theta^2 & 0 \\ S_{2\theta} & 0 & 0 & S_{2\theta} & 0 & -2S_\theta^2 & 2S_\theta^2 & 0 \\ 0 & 0 & 0 & 0 & 0 & 0 & 0 & 0 \end{bmatrix} \tag{3.25}$$

where $A = 4+6d\bar{w}+3d^2\bar{w}^2-d\bar{w}(2+d\bar{w})C_{2\theta}$. We, therefore, characterize nonlocal correlations in the above state by optimizing expectation values of $|M_{cum}|$ and $|S_{cum}|$ with respect to all parameters involved. Figure 3.6(a) and Figure 3.6(b) describe the importance of weak measurement and its

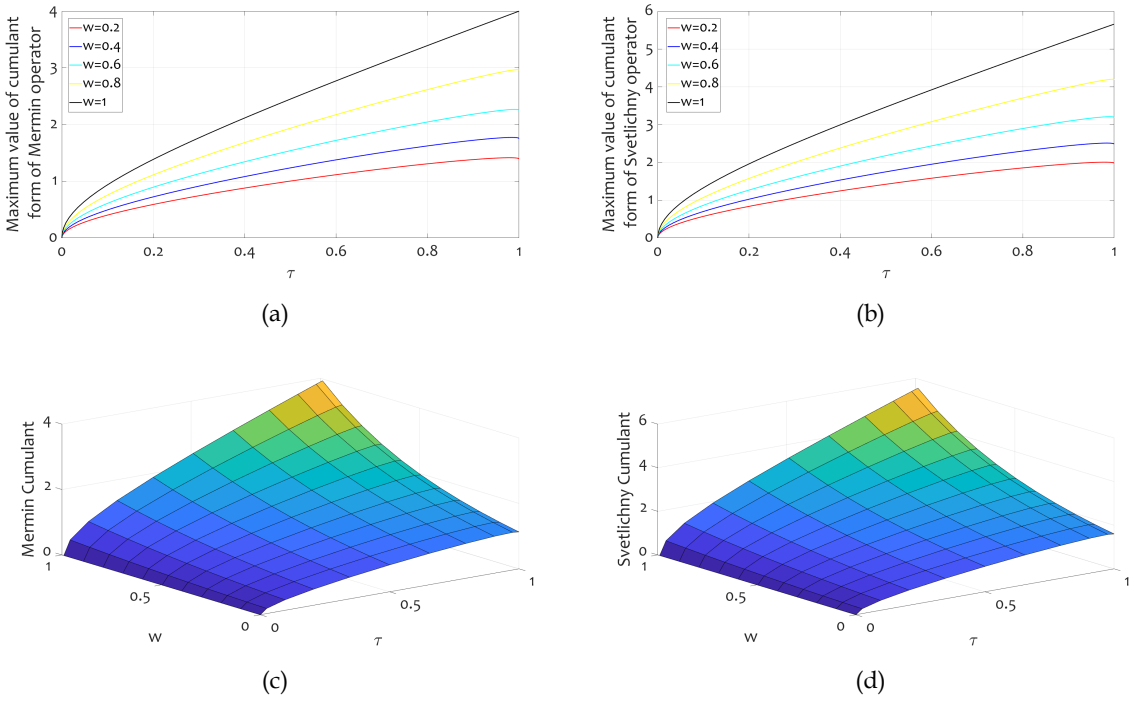

Figure 3.6 : Effects of weak measurement operations on the nonlocality of $|\Phi\rangle$ states using (a), (c) $|M_{cum}|$ and (b), (d) $|S_{cum}|$ operators

reversal operations in retrieving the original nonlocal correlations in $|\Phi\rangle$ states. Surprisingly, unlike the case of *GGHZ* states in presence of noise and weak measurements, here the set of partially entangled states exhibiting higher nonlocal correlations than the maximally entangled input *GHZ* state is substantially less. Precisely, the non-coincidence of nonlocality-in smaller set of partially entangled states- with entanglement of the original state also vanishes for larger values of the weak measurement operator as evident from Figure 3.6(a) and Figure 3.6(b). A comparison of Figure 3.5 and Figure 3.6 at $d = 0.7$ clearly shows that even at moderate strengths of weak measurement parameter, nonlocal correlations in $|\Phi\rangle$ states increase substantially.

3.5 NONLOCALITY IN *MS* STATES

Now, we extend our discussion to analyze nonlocal properties of yet another efficient set of three-qubit entangled states, *MS* states [Carteret and Sudbery, 2000], represented as

$$|\psi_{MS}\rangle = \frac{1}{\sqrt{2}}(|000\rangle + Cos(\theta_{MS})|110\rangle + Sin(\theta_{MS})|111\rangle) \tag{3.26}$$

where $0 < \theta_{MS} \leq \frac{\pi}{2}$. The set of partially entangled *MS* states have been extensively studied and used as entangled resources in quantum information processing protocols [Liu *et al.*, 2016; Wei *et al.*, 2018b; Zhou *et al.*, 2019]. Considering that these states also belong to the *GHZ* class, one can characterize the degree of entanglement in *MS* states using three-tangle (τ) as an entanglement measure. The three-tangle for $|\psi_{MS}\rangle$ states is $\tau(|\psi_{MS}\rangle) = Sin^2(\theta_{MS})$ indicating that the set of states are entangled for the complete range of state parameter with $\tau = 1$ for the maximally entangled *GHZ* state. One can see that the value of three-tangle for *MS* states is distinctly different from the values of τ obtained for *GGHZ* and $|\Phi\rangle$ states. Nevertheless, the nature and properties of three-qubit entanglement are similar in all three cases.

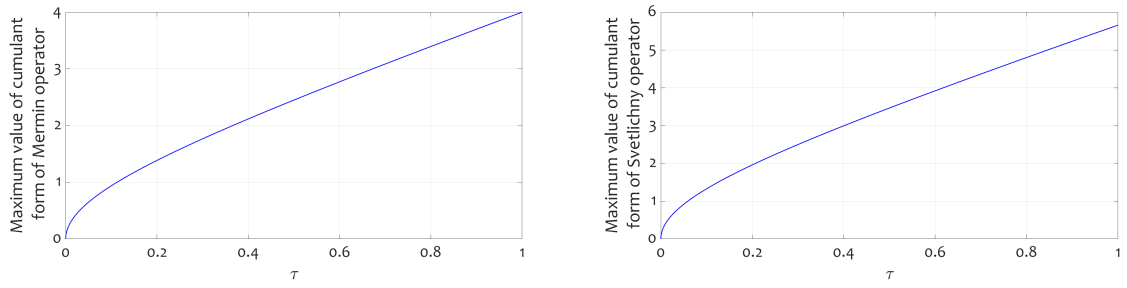

(a) (b)

Figure 3.7 : Maximum expectation values of (a) $|M_{cum}|$, (b) $|S_{cum}|$ operators versus three-tangle (τ) for *MS* states

We further evaluate optimal expectation values of modified Mermin and Svetlichny operators for $|\psi_{MS}\rangle$ states to establish a relation between nonlocality and entanglement measure or the state parameter. Figure 3.7 confirms that nonlocality in *MS* states using $|M_{cum}|$ and $|S_{cum}|$ operators monotonically increases with the increase in degree of entanglement τ. Similar to the previous cases, *MS* states also violate $|M_{cum}|$ and $|S_{cum}|$ inequalities maximally for the maximally entangled GHZ state. Interestingly, nonlocal correlations in *MS* and $|\Phi\rangle$ states are same but different in comparison to the *GGHZ* states. A comparison clearly shows that *GGHZ* states exhibit more nonlocal correlations for the complete range of τ in comparison to *MS* and $|\Phi\rangle$ states.

3.5.1 Nonlocality in *MS* states in presence of noise and weak measurements

Similar to our discussions for *GGHZ* and $|\Phi\rangle$ states, here also we analyze nonlocality in *MS* states in noisy environment considering strengths of amplitude damping channels and weak measurements for all three qubits to be the same. We obtain maximum expectation values of $|M_{cum}|$ and $|S_{cum}|$ operators for *MS* states in presence of noise and weak measurements by optimizing these values for all parameters and using the optimal relation between the noise parameter and weak measurement parameters. The density operators corresponding to the evolved mixed states in noisy conditions with absence and presence of weak measurement operators are represented in the Appendix.

We represent effects of decoherence on nonlocal correlations of *MS* states using modified Mermin and Svetlichny inequalities in Figure 3.8(a) and Figure 3.8(b), respectively. Although, *MS*

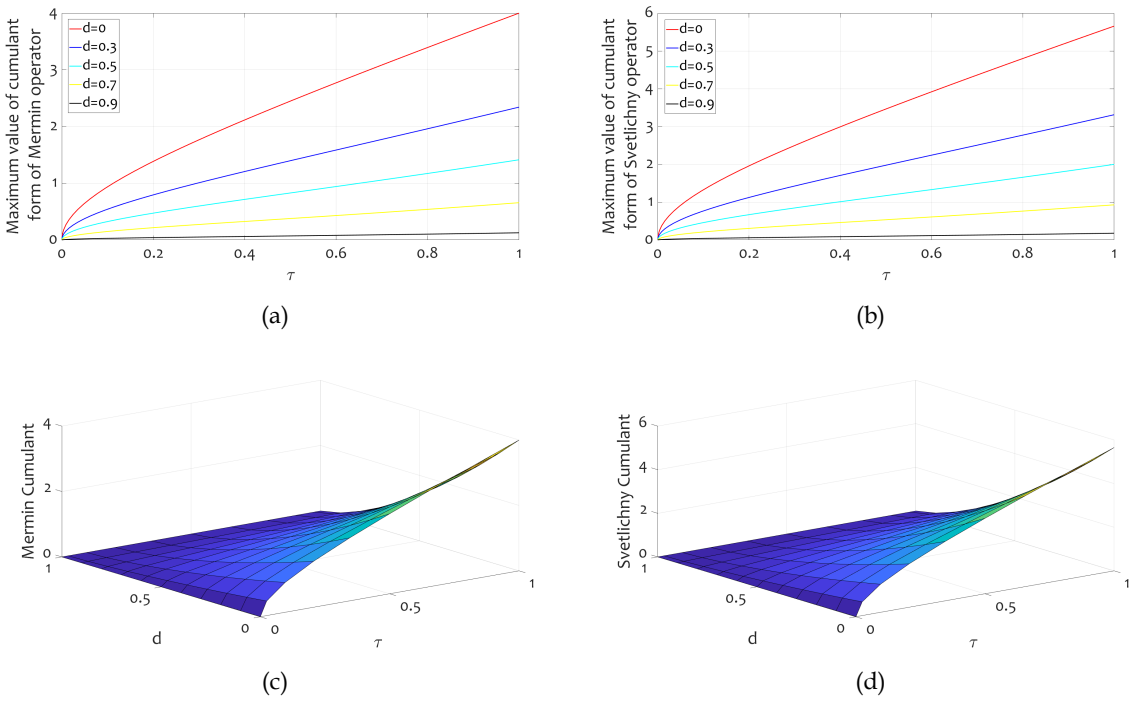

Figure 3.8 : Effects of amplitude damping noise on the nonlocality of MS states using (a), (c) $|M_{cum}|$ and (b), (d) $|S_{cum}|$ operators

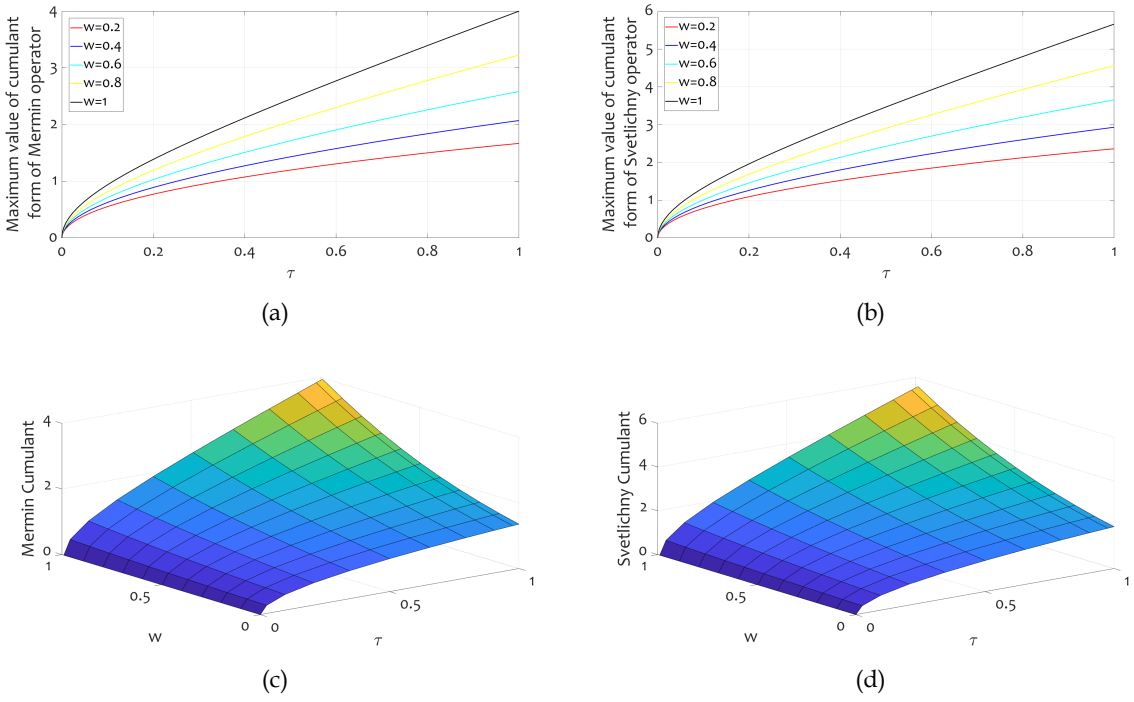

Figure 3.9 : Effects of weak measurement operations on the nonlocality of MS states using (a), (c) $|M_{cum}|$ and (b), (d) $|S_{cum}|$ operators

states are relatively robust against the amplitude damping noise in comparison to $|\Phi\rangle$ states, the nature of degradation of nonlocal correlations in presence of amplitude damping channels in both cases is same. A comparison of the three sets of GHZ class states discussed in this chapter reveals that $GGHZ$ states are the most robust in presence of the amplitude damping noise, similar to our

discussion in the ideal case. Moreover, nonlocal correlations consistently increase from $\tau = 0$ to $\tau = 1$ for all values of the noise parameter except when the strength of noise parameter approaches its maximum value.

Figure 3.9(a) and Figure 3.9(b) illustrate effects of weak measurement and its reversal operations considering the decoherence parameter $d = 0.7$ on $|M_{cum}|$ and $|S_{cum}|$ operators, respectively. A comparison of figures depicting effects of noise on modified operators in absence and presence of weak measurements clearly demonstrates the effectiveness of the technique to preserve quantum correlations. Although the retrieval of nonlocal correlations for a particular w is better in *MS* states as against the case of $|\Phi\rangle$ states, *GGHZ* states are clearly the best owing to the properties of nonlocal correlations in presence and absence of noise. The agreement between nonlocality and degree of entanglement of the original input state for all values of the weak measurement parameter w clearly suggests that properties of *MS* states are distinctly different from that of *GGHZ* and $|\Phi\rangle$ states. One can easily observe the one-to-one correspondence between nonlocality and entanglement of original state for *MS* states unlike our discussions in *GGHZ* states and $|\Phi\rangle$ states where nonlocality does not always coincide with the entanglement of input state in presence of weak measurement operations.

3.6 NONLOCALITY IN *W* STATES

Dür *et al.* [Dür *et al.*, 2000] have demonstrated that three-qubit entangled pure states can be characterized into two different inequivalent classes, namely, *GHZ* class and *W* class. The two sets of states cannot be transformed to one another with non-zero probability using local operations and classical communication (LOCC). The entanglement properties of two sets of states are distinctly different as can be seen from the reduced density operators of both classes if one of the qubits is traced out [Dür *et al.*, 2000]. Similar to *GGHZ*, *MS*, and $|\Phi\rangle$ states, the *W* class of states are extensively studied in literature and have been efficiently used for quantum information and computation [Joo *et al.*, 2003; Li and Qiu, 2007; Jian *et al.*, 2007; Li *et al.*, 2008; Chen *et al.*, 2008; Li *et al.*, 2009; Hwang *et al.*, 2011; Hao *et al.*, 2011; Liu *et al.*, 2011, 2012a; Tsai *et al.*, 2019]. Here, we define a class of three-qubit pure entangled states, *W* states, given as

$$|\psi_W\rangle = Sin(\theta_W)|001\rangle + \frac{Cos(\theta_W)}{\sqrt{2}}(|100\rangle + |010\rangle) \tag{3.27}$$

where $0 < \theta_W \leq 0.6155\ rad$. The set of $|\psi_W\rangle$ states represent the general *W* class with $a = Sin\theta_W$, and $b = c = \frac{Cos\theta_W}{\sqrt{2}}$. For $\theta_W = 0.6155\,rad$, $|\psi_W\rangle$ states represent the standard three-qubit *W* state. The set of *GGHZ* and *W* states can be distinguished from each other using the three-qubit entanglement measure τ. Precisely, three-tangle is defined in a way such that it has non-zero values for all states in *GHZ* class, whereas three-tangle for *W* class of states turns out to be 0. For example, the three-tangle as also discussed in previous sections- for *GGHZ*, $|\Phi\rangle$, and *MS* states are $Sin^2(2\theta)$, $Sin^2(2\theta_\Phi)$, and $Sin^2(\theta_{MS})$ respectively, but for the standard three-qubit *W* states, $\tau = 0$. The degree of entanglement in *W* class can be measured using different ways, e.g., by computing the average entanglement in all bipartite mixed states [Dür *et al.*, 2000]. Alternately, one can use σ [Emary and Beenakker, 2004] to measure the degree of entanglement in *W* class of states as defined in Eq. (1.28) expressed in Chapter 1. We, therefore, evaluate σ for $|\psi_W\rangle$ as $\sigma(|\psi_W\rangle) = min\{\frac{1}{4}Cos^2\theta_W(3 - Cos2\theta_W), \frac{1}{2}Sin^2 2\theta_W\}$. Hence, the degree of entanglement in *W* states increases for all $\theta > 0$ and the maximum entanglement $\sigma(|\psi_W\rangle) = \frac{4}{9}$ corresponds to the standard three-qubit *W* state for $\theta_W = 0.6155\,rad$. Figure 3.10 shows the violation of modified Mermin and Svetlichny inequalities by all states represented in Eq. (3.27) for all $\sigma > 0$. The maximum violation for $|M_{cum}|$ and $|S_{cum}|$ inequalities are 1.9397 and 2.754, respectively. This is in contrast to the *GGHZ* class of states where the maximum violation reaches a value of 4 and $4\sqrt{2}$ for $|M_{cum}|$ and $|S_{cum}|$, respectively. The high values of nonlocal correlations using modified operators further confirm the importance of *GHZ* class of states as against the *W* class of states for three-qubit pure entangled systems. Similar to

the *GHZ* class, $|\psi_W\rangle$ states also show higher violation for the modified Svetlichny inequality in comparison to the modified Mermin inequality.

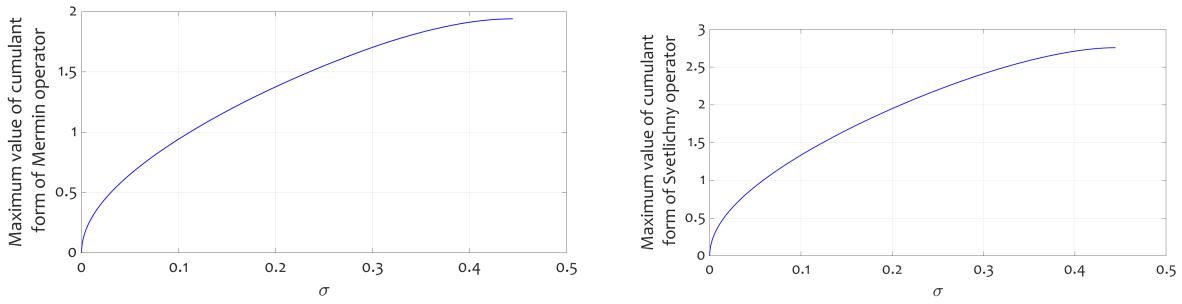

(a) (b)

Figure 3.10 : Maximum expectation values of (a) $|M_{cum}|$, (b) $|S_{cum}|$ operators versus σ for W states

3.6.1 Nonlocality of W states in presence of noise and weak measurements

In this subsection, we now proceed to analyze nonlocality of W states using modified operators in presence of noise with and without applications of weak measurement and its reversal operations. As earlier, we consider strengths of amplitude damping channels and weak measurement operations to be the same for all three qubits. The corresponding mixed state density operators associated with evolved states through noisy channels in absence and presence of weak measurements are represented as follows:

$$\rho_W^{AD} = \frac{1}{2\sqrt{2}} \begin{bmatrix} 2\sqrt{2}d & 0 & 0 & 0 & 0 & 0 & 0 & 0 \\ 0 & 2\sqrt{2}\bar{d}S_\theta^2 & \bar{d}S_{2\theta} & 0 & \bar{d}S_{2\theta} & 0 & 0 & 0 \\ 0 & \bar{d}S_{2\theta} & \sqrt{2}\bar{d}C_\theta^2 & 0 & \sqrt{2}\bar{d}C_\theta^2 & 0 & 0 & 0 \\ 0 & 0 & 0 & 0 & 0 & 0 & 0 & 0 \\ 0 & \bar{d}S_{2\theta} & \sqrt{2}\bar{d}C_\theta^2 & 0 & \sqrt{2}\bar{d}C_\theta^2 & 0 & 0 & 0 \\ 0 & 0 & 0 & 0 & 0 & 0 & 0 & 0 \\ 0 & 0 & 0 & 0 & 0 & 0 & 0 & 0 \\ 0 & 0 & 0 & 0 & 0 & 0 & 0 & 0 \end{bmatrix} \tag{3.28}$$

and

$$\rho_W^{ADWM} = \frac{1}{2\sqrt{2}(1+d\bar{w})} \begin{bmatrix} 2\sqrt{2}d\bar{w} & 0 & 0 & 0 & 0 & 0 & 0 & 0 \\ 0 & 2\sqrt{2}S_\theta^2 & S_{2\theta} & 0 & S_{2\theta} & 0 & 0 & 0 \\ 0 & S_{2\theta} & \sqrt{2}C_\theta^2 & 0 & \sqrt{2}C_\theta^2 & 0 & 0 & 0 \\ 0 & 0 & 0 & 0 & 0 & 0 & 0 & 0 \\ 0 & S_{2\theta} & \sqrt{2}C_\theta^2 & 0 & \sqrt{2}C_\theta^2 & 0 & 0 & 0 \\ 0 & 0 & 0 & 0 & 0 & 0 & 0 & 0 \\ 0 & 0 & 0 & 0 & 0 & 0 & 0 & 0 \\ 0 & 0 & 0 & 0 & 0 & 0 & 0 & 0 \end{bmatrix} \tag{3.29}$$

Figure 3.11 reflects properties of nonlocal correlations of W states in presence of amplitude damping noise. Although the nature of degradation of nonlocal correlations is same as in the case of *GGHZ* states, considering that the decrease in nonlocality is more rapid in case of W class states, the *GGHZ* states are clearly more robust against the amplitude damping noise in comparison to the W class states. Similar to the states in *GHZ* class, W class states also show an agreement between nonlocality in presence of noise and the degree of entanglement of the original input state. In order

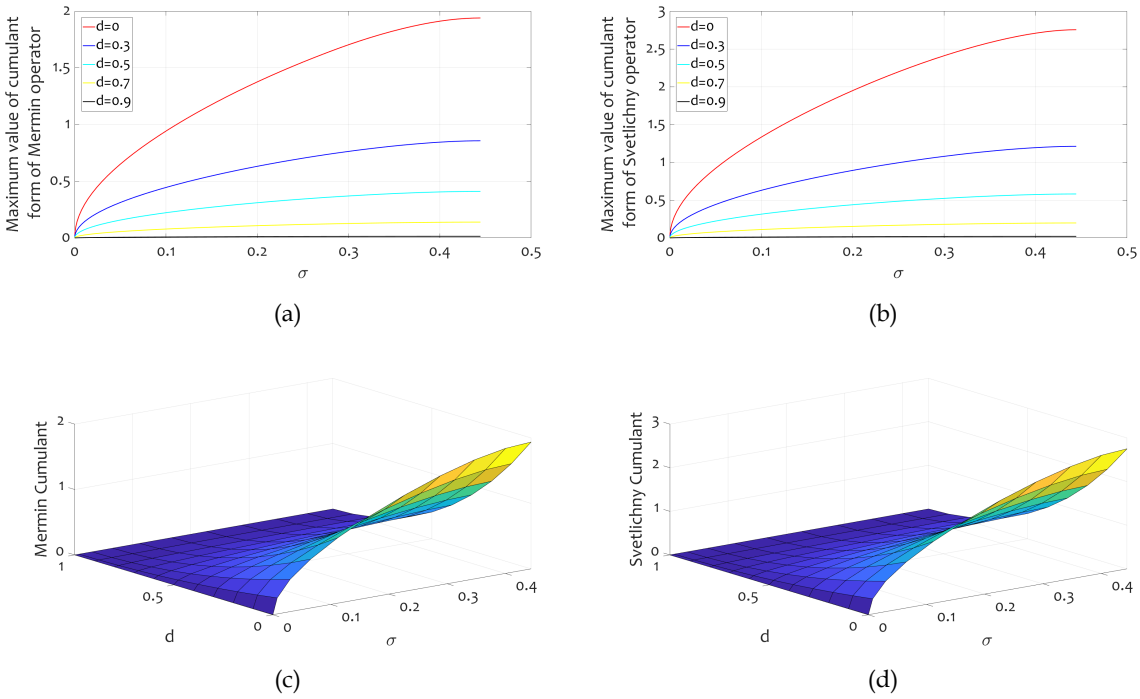

Figure 3.11 : Effects of amplitude damping noise on the nonlocality of W states using (a), (c) $|M_{cum}|$ and (b), (d) $|S_{cum}|$ operators

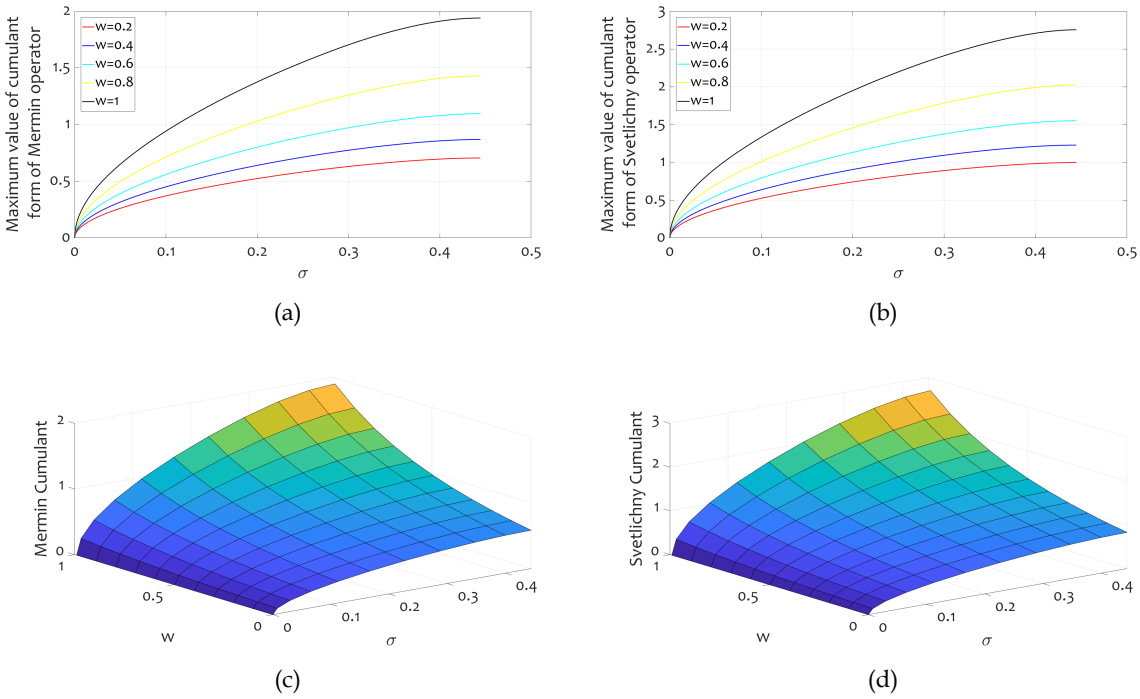

Figure 3.12 : Effects of weak measurement operations on the nonlocality of W states using (a), (c) $|M_{cum}|$ and (b), (d) $|S_{cum}|$ operators

to preserve quantum correlations in W class states, as earlier, we find a correspondence between the optimal expectation value of $|M_{cum}|$ and $|S_{cum}|$ operators with weak measurement operators in presence of the amplitude damping noise. Figure 3.12 shows increase in nonlocal correlations with the increase in weak measurement parameter strength following an optimal relation between

noise and weak measurement parameters to optimize correlations in presence of noise. Unlike the *GGHZ* and $|\Phi\rangle$ states and similar to the case of *MS* states, for *W* class states nonlocality coincides with the three-qubit entanglement measure σ for all values of the weak measurement parameter.

3.7 NONLOCALITY IN W_N STATES

In general, the use of partially entangled states in comparison to use of maximally entangled states results in less efficiency of a protocol in quantum information and computation, at least in the ideal conditions [Joo *et al.*, 2003]. For example, the use of partially entangled three-qubit standard *W* state results in fidelity of teleportation dependent on the parameters of the state to be teleported, and the obtained fidelity is obviously less than the unity [Shi and Tomita, 2002]. All the states of *W* class are partially entangled three-qubit pure states with the standard *W* state exhibiting the maximum entanglement, therefore, use of any of the *W* states as entangled resources leads to a probabilistic teleportation protocol. On the other hand, Agrawal and Pati [Agrawal and Pati, 2006] proposed a special set of W_n states which can be used as resources for perfect teleportation and dense coding. The set of W_n states have been shown to be useful in quantum information and computation and considering its importance for quantum information processing, these set of states have been also realized experimentally [Dong *et al.*, 2016]. Moreover, a *N*-qubit generalization of W_n states have also been studied for its efficacy in quantum information and computation with a proposal to experimentally prepare the four-qubit W_n states [Singh *et al.*, 2016]. Therefore, in this section, we consider three-qubit W_n states proposed by Agrawal and Pati [Agrawal and Pati, 2006] for analyzing nonlocal correlations in these states using our modified operators. For this, we represent W_n states as

$$|W_n\rangle = \frac{1}{\sqrt{2+2n}}(|100\rangle + \sqrt{n}e^{i\gamma}|010\rangle + \sqrt{n+1}e^{i\delta}|001\rangle). \tag{3.30}$$

where γ and δ are relative phases and n is a positive integer. As these states belong to *W* class of states, three-tangle (τ) for $|W_n\rangle$ states is zero. Thus, we evaluate the degree of entanglement in $|W_n\rangle$ states using σ [Emary and Beenakker, 2004] as $\sigma(|W_n\rangle) = \frac{1+2n}{2(1+n)^2}$. The value for σ suggests that the degree of entanglement in W_n states decreases as n increases. For example, for $n = 1$ and $\gamma = \delta = 0$, $|W_1\rangle$ state represented as

$$|W_1\rangle = \frac{1}{2}(|100\rangle + |010\rangle + \sqrt{2}|001\rangle), \tag{3.31}$$

show maximum value for σ, i.e., $\sigma(|W_1\rangle) = \frac{3}{8} = 0.375$. Although $|W_1\rangle$ state exhibits maximum entanglement among all $|W_n\rangle$ states, the degree of entanglement in $|W_1\rangle$ states is still substantially less than the one observed for the standard three-qubit *W* state, i.e., $\sigma(W) = \frac{4}{9} = 0.444$. For characterizing nonlocal correlations in W_n states, we considered $n \in [1, 11]$. Figure 3.13 suggests that all W_n states violate our inequalities suggesting the existence of genuine nonlocal correlations between three qubits. As n increases, the violation of both inequalities decreases and for larger values of n the violation is also very less. The decrease in nonlocal correlations, however, is in line with the decrease in the entanglement measure σ with the decreasing n. Interestingly or rather surprisingly, in contrast to all pure three-qubit entangled states discussed previously in this chapter where entanglement and nonlocal correlations increase with increasing value of the state parameter, for W_n states both entanglement and nonlocality decrease with increasing value of the state parameter. The violation of $|M_{cum}|$ and $|S_{cum}|$ inequalities ranges from 1.7321 to 0.8347 for $|M_{cum}|$ and 2.4495 to 1.1807 for $|S_{cum}|$, respectively where the maximum and minimum values correspond to $n = 1$ and $n = 11$. Although the standard *W* state possess more entanglement and nonlocal correlations than any of the W_n states, W_n states are found to be more useful than the standard *W* states. This further indicates towards the complex relations between entanglement, nonlocality and efficacy of quantum resources for quantum information and computation.

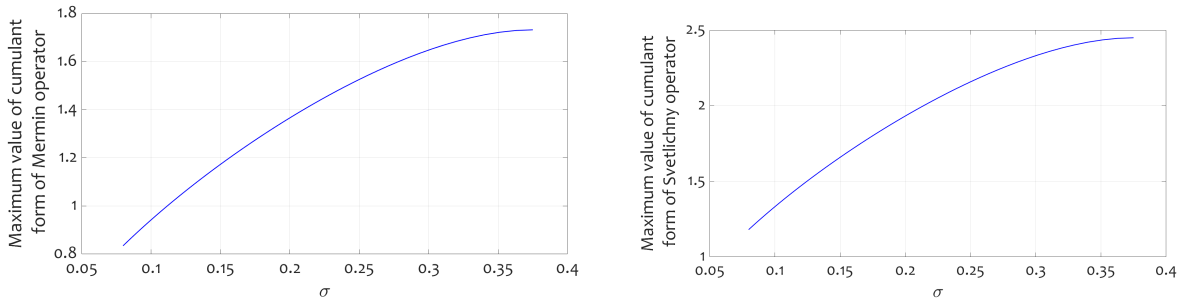

(a) (b)

Figure 3.13 : Maximum expectation values of (a) $|M_{cum}|$, (b) $|S_{cum}|$ operators versus σ for W_n states

3.7.1 Nonlocality of W_n states in presence of noise and weak measurements

Considering same strengths of noise and weak measurement parameters for all three qubits, in Figure 3.14(a) and Figure 3.14(b), we show effects of decoherence on the nonlocal correlations of W_n states as identified by $|M_{cum}|$ and $|S_{cum}|$, respectively. In comparison to W states, W_n states are less robust against amplitude damping channels. The behavior of nonlocal

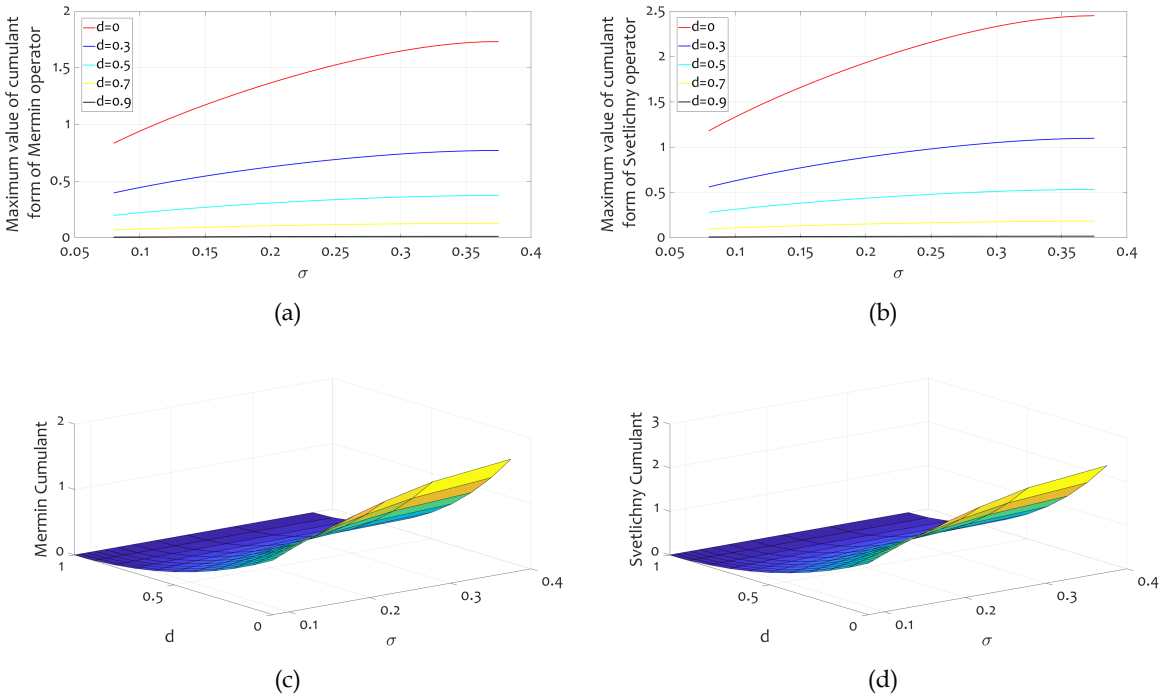

Figure 3.14 : Effects of amplitude damping noise on the nonlocality of W_n states using (a), (c) $|M_{cum}|$ and (b), (d) $|S_{cum}|$ operators

correlations in presence of noise, however, is the same in both sets of states. W_1 states still correspond to the maximum violation of $|M_{cum}|$ and $|S_{cum}|$ inequalities even in presence of noise. Figure 3.15 further demonstrates effects of weak measurements on W_n states in presence of noise. The results are similar to the one obtained for the W class states. The maximum nonlocality corresponds to the maximally entangled input state, i.e. W_1, irrespective of the strength of weak measurement parameter.

So far, we have analyzed nonlocal correlations in three-qubit pure entangled states using our operators. In the next section, we proceed to discuss nonlocality in few classes of three-qubit

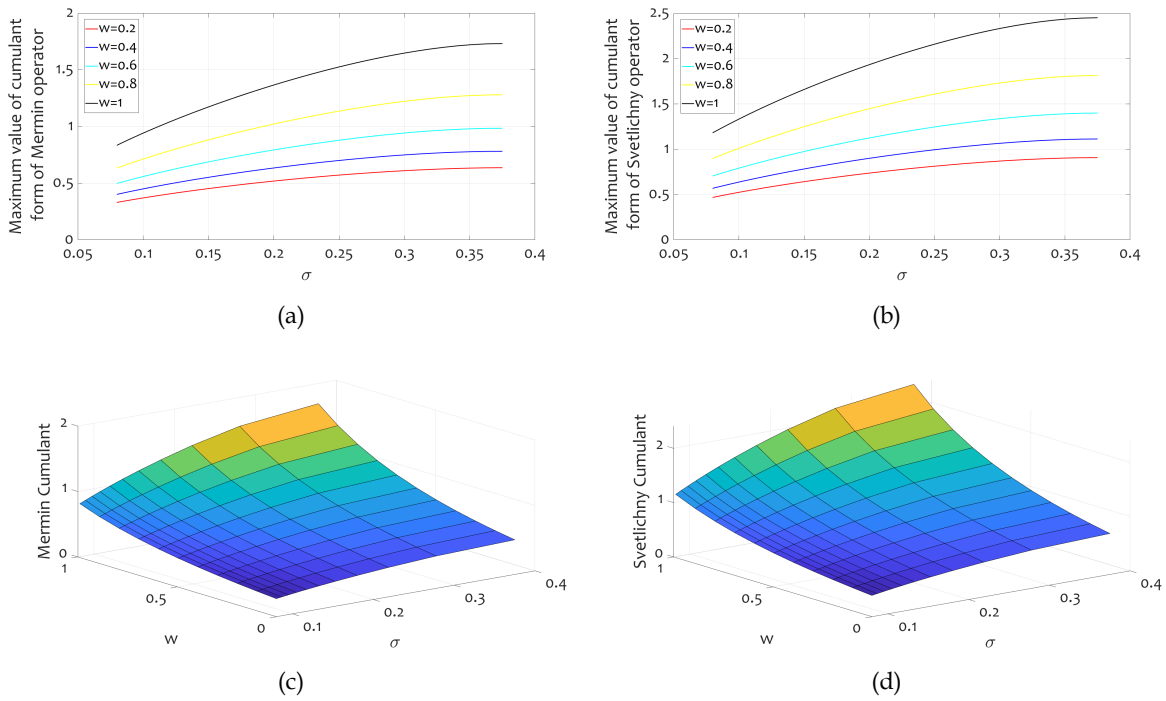

Figure 3.15 : Effects of weak measurement operations on the nonlocality of W_n states using (a), (c) $|M_{cum}|$ and (b), (d) $|S_{cum}|$ operators

mixed entangled states in presence and absence of amplitude damping channels.

3.8 NONLOCALITY IN MIXED STATES

In order to extend our analysis from pure to mixed states, we consider following three sets of mixed states, namely
(i) a mixture of *GHZ* state with white noise [Eltschka and Siewert, 2012],
(ii) a mixture of *W* state with white noise [Zhao *et al.*, 2013], and
(iii) a state with convex sum of projectors onto a *GHZ* state and a *W* state [Lohmayer *et al.*, 2006] given as

$$(i)\ \rho_a = a\,|\psi_{GHZ}\rangle\langle\psi_{GHZ}| + \frac{(1-a)}{8}I, \tag{3.32}$$

$$(ii)\ \rho_b = b\,|\psi_W\rangle\langle\psi_W| + \frac{(1-b)}{8}I, \text{ and} \tag{3.33}$$

$$(iii)\ \rho_c = c\,|\psi_{GHZ}\rangle\langle\psi_{GHZ}| + (1-c)\,|\psi_W\rangle\langle\psi_W|, \tag{3.34}$$

respectively, where a, b, c are state parameters, and $|\psi_{GHZ}\rangle = \frac{1}{\sqrt{2}}(|000\rangle + |111\rangle)$, and $|\psi_W\rangle = \frac{1}{\sqrt{3}}(|001\rangle + |010\rangle + |100\rangle)$ are maximally entangled *GHZ* and standard *W* states. Although one can evaluate the degree of entanglement of states represented above using three-tangle for mixed states but the minimization procedure over all possible ensembles of pure states makes it relatively difficult [Uhlmann, 2000; Jung *et al.*, 2009]. Thus, here we use tripartite-negativity [Sabín and García-Alcaine, 2008] as an entanglement measure for these three mixed states such that

$$N(\rho_a) = Max[0, \frac{1}{4}(-1+5a)],$$

$$N(\rho_b) = Max[0, \frac{1}{12}(-3+b(3+8\sqrt{2}))], \text{ and}$$

$$N(\rho_c) = \frac{1}{6}(-2-c+2\sqrt{1-2c+10c^2}+\sqrt{32-64c+41c^2}). \tag{3.35}$$

Figure 3.16 suggests that ρ_c is entangled for complete range of the state parameter c and exhibits higher entanglement in comparison to other two states. Moreover, both ρ_a and ρ_b are entangled only after state parameters a and b exceed a certain value. For example ρ_a and ρ_b are entangled iff $a > 0.2$ and $b > \frac{3}{3+8\sqrt{2}}$, respectively. In all other ranges of the parameters a and b, the states are considered to be separable. The nature of entanglement in all mixed states clearly reflects the properties of the mixtures represented above. For nonlocal correlations in mixed states, Figure 3.17

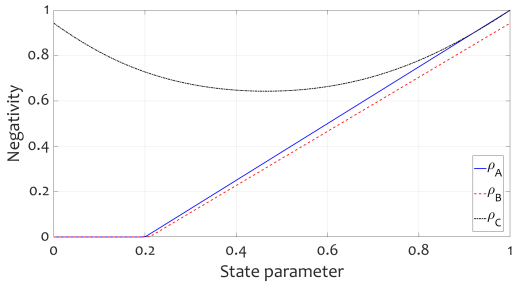

Figure 3.16 : Negativity ($N(\rho)$) versus state parameters of mixed states

suggests that all three sets of mixed states violate modified Mermin and Svetlichny inequalities. The states ρ_a and ρ_b exhibit nonlocal correlations even for $a < 0.2$ and $b < \frac{3}{3+8\sqrt{2}}$ suggesting that such states can also be useful in quantum information and computation. This can also be verified using the global quantum discord [Rulli and Sarandy, 2011] which shows the presence of quantumness in the system for all values of state parameters. For example, in the mixed state ρ_a, for all values of $a > 0$, global quantum discord is greater than 0 and at $a = 1$, it is 1 [Rulli and Sarandy, 2011]. For

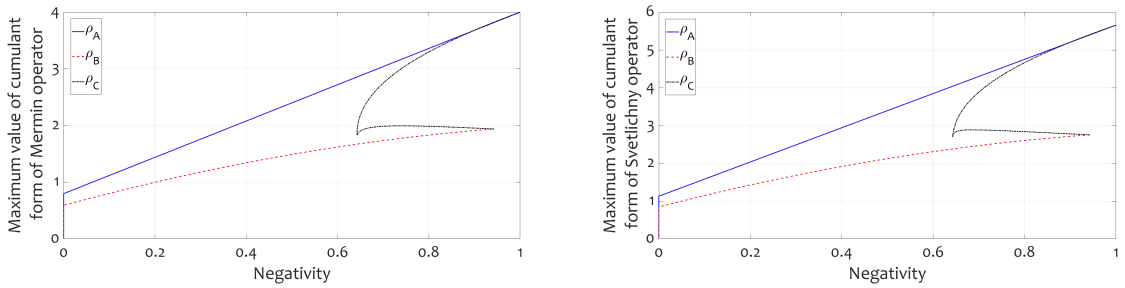

(a) (b)

Figure 3.17 : Maximum expectation values of (a) $|M_{cum}|$, (b) $|S_{cum}|$ operators versus negativity ($N(\rho)$) for mixed states

$a = 1$ and $b = 1$, ρ_a and ρ_b lead to the maximally entangled GHZ and standard W states, respectively, and therefore violate the inequality maximally for those values. Considering that ρ_c is a convex linear combination of GHZ and W states, we get minimum violation corresponding to the standard W state for $c = 0$ and maximum violation corresponding to the maximally entangled GHZ state for $c = 1$ in both cases as shown in Figure 3.17(a) and Figure 3.17(b).

3.8.1 Nonlocality of mixed states in presence of noise

In this subsection, we use one of the mixed states ρ_a represented in Eq. (3.32) for analyzing nonlocal correlations using our operators in the presence of noise. The analysis in other two cases are exactly the same and we get results of similar nature. Considering same strength of amplitude damping channels for all three-qubits, Figure 3.18(a) and Figure 3.18(b) describe the degradation of quantum correlations with increasing strength of the noise parameter. Consistent with the

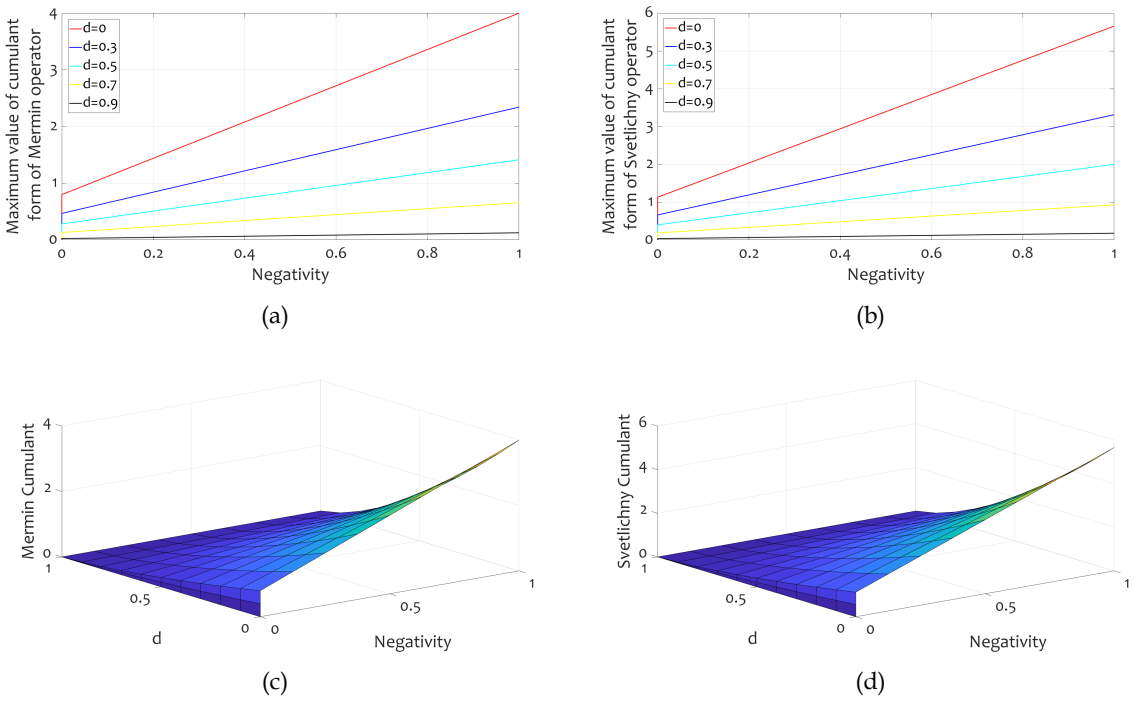

Figure 3.18 : Effects of amplitude damping noise on the nonlocality of mixed states using (a), (c) $|M_{cum}|$ and (b), (d) $|S_{cum}|$ operators

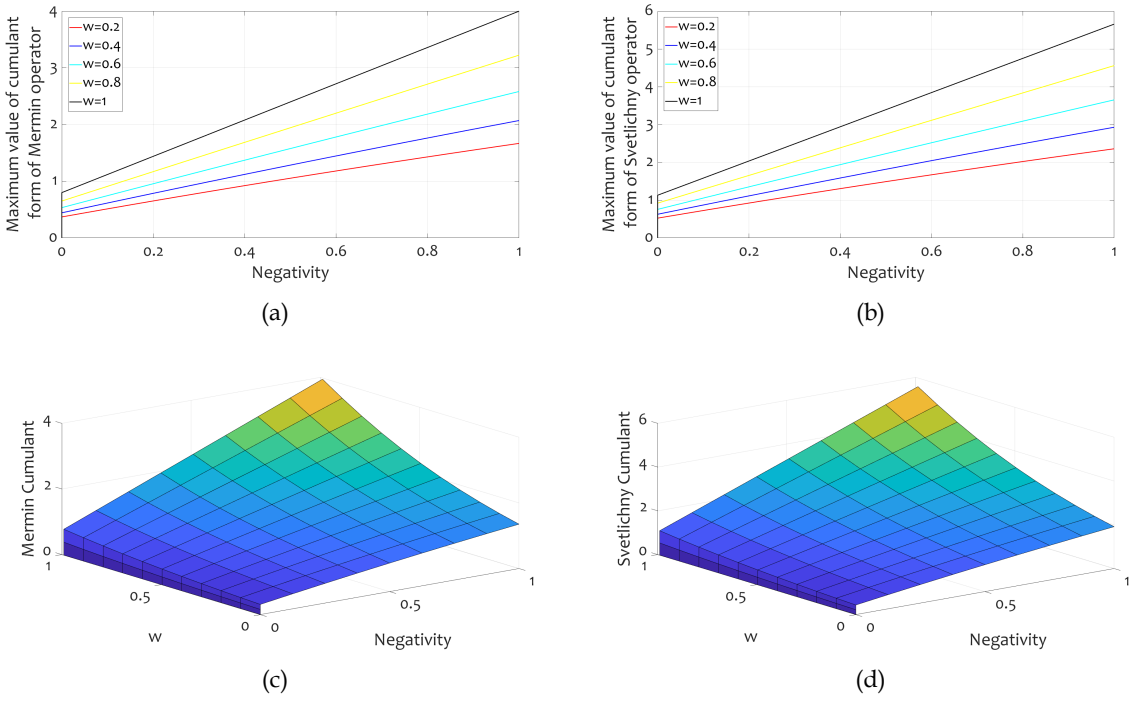

Figure 3.19 : Effects of weak measurement operations on the nonlocality of mixed states using (a), (c) $|M_{cum}|$ and (b), (d) $|S_{cum}|$ operators

structure of mixed state, for lower values of entanglement measure, ρ_a displays more quantum correlations even in comparison to pure states such as $|\Phi\rangle$ and MS states. However, $GGHZ$ states show higher correlations than ρ_a. Moreover, the set of states possess nonlocal correlations even in presence of noise for the range where the original state is a separable state.

Finally, we consider applications of weak measurement and reversal operations for reducing the effect of noise on the nonlocal properties of three-qubit mixed states where we consider same strengths of weak measurement parameters and decoherence parameters for all three-qubits; and value of decoherence parameter as $d = 0.7$. Figure 3.19(a) and Figure 3.19(b) further show one-to-one correspondence between nonlocality and entanglement of the original state. Similar observations can be made for other mixed states as well.

3.9 NONLOCALITY OF THREE QUBIT STATES IN PRESENCE OF DEPOLARIZING NOISE

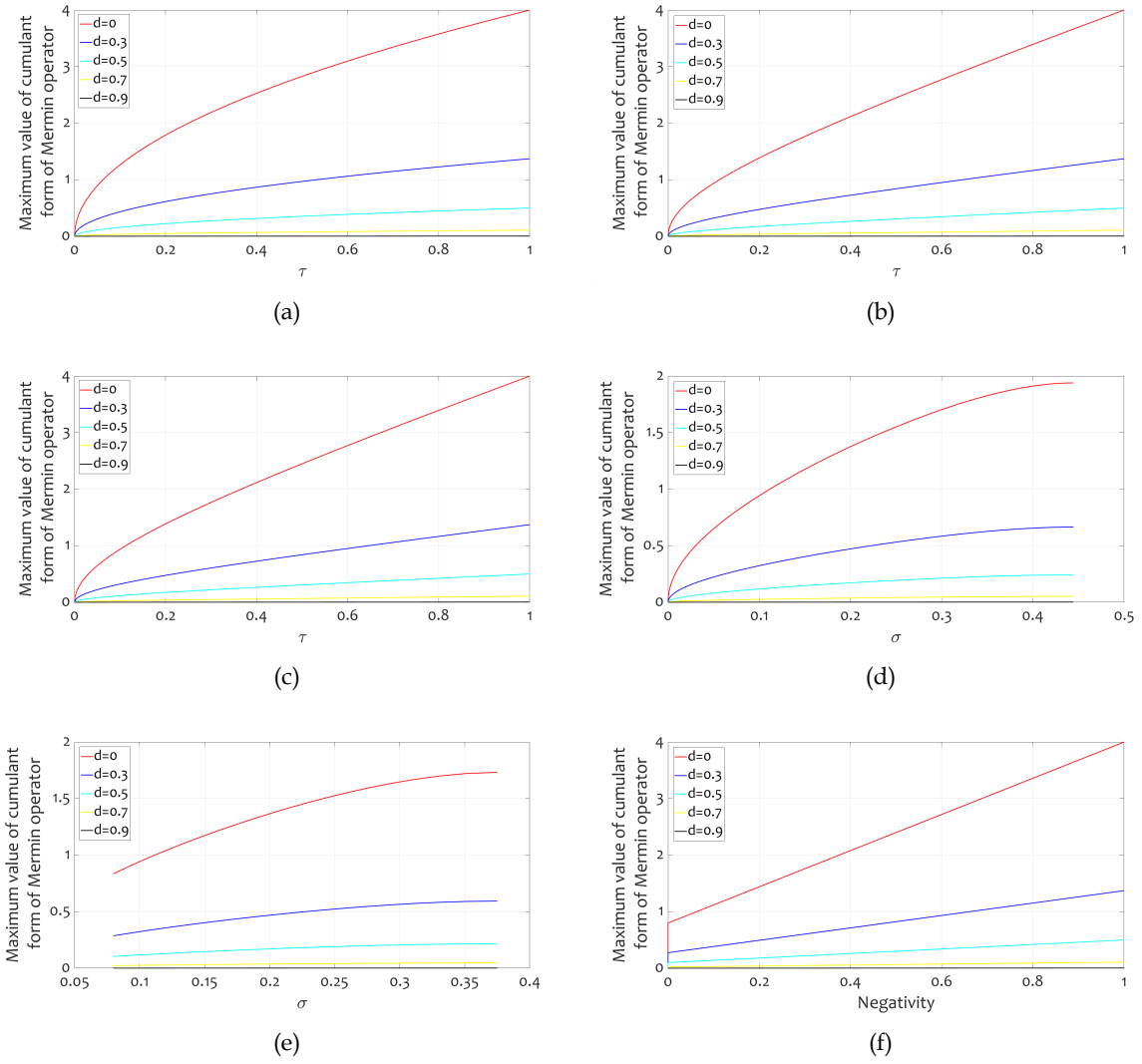

Figure 3.20 : Effects of depolarizing noise on the nonlocality of (a) $GGHZ$, (b) $|\Phi\rangle$, (c) MS, (d) W, (e) W_n and (f) mixed states using $|M_{cum}|$ operator

In this section, we extend our discussion to analyze effects of a depolarizing channel on nonlocal correlations as discussed using modified Mermin and Svetlichny operators. Similar to the case of amplitude damping channels, we further consider the strengths of depolarizing channels to be same for all three qubits. Figure 3.20 and Figure 3.21 demonstrate the results of the original state passing through depolarizing channels. In comparison to the amplitude damping noise, nonlocal correlations decay much more faster in case of depolarizing noise confirming the detrimental effects of depolarizing channels for all pure and mixed states discussed in this chapter. In the presence of depolarizing noise, within the GHZ class of states, $GGHZ$ states are most robust in

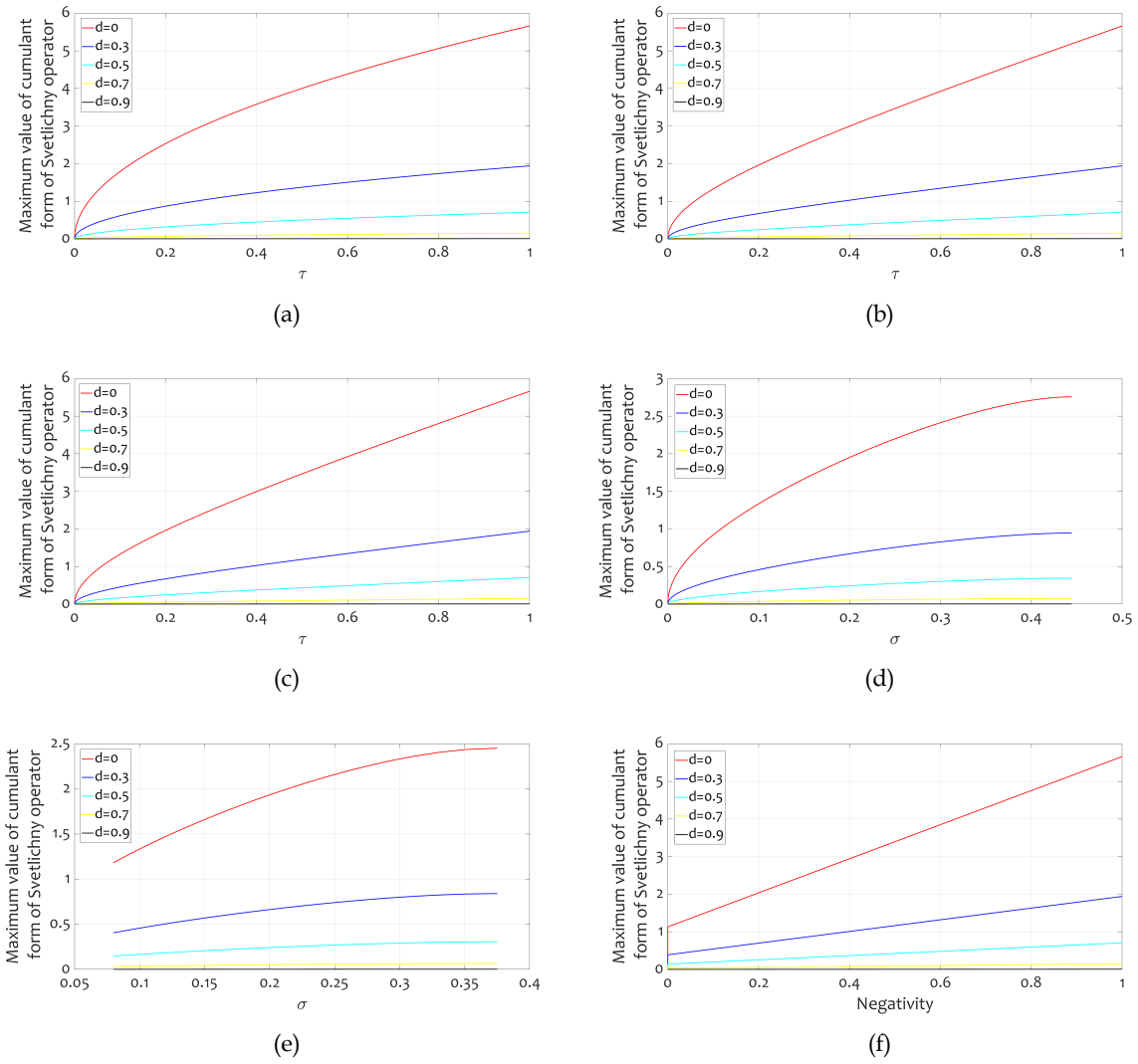

Figure 3.21 : Effects of depolarizing noise on the nonlocality of (a) $GGHZ$, (b) $|\Phi\rangle$, (c) MS, (d) W, (e) W_n and (f) mixed states using $|S_{cum}|$ operator

comparison to MS and $|\Phi\rangle$ states. The effect of depolarizing noise, however, is same for both MS and $|\Phi\rangle$ states. For W class states, the adverse effects of noise are almost the same for W and W_n states. Similar to our discussions on the amplitude damping noise, here also our results do not lead to disagreement between nonlocality and entanglement of the original input state.

3.10 SUMMARY

In this chapter, we revisited the question of analyzing genuine nonlocal correlations in pure and mixed three qubit states in presence of noise and weak measurement operations. The identification of genuine nonlocal correlations in multiqubit systems is imperative if one wants to create an efficient quantum network among different users in the protocol. Genuine multiqubit entanglement and nonlocality is of profound interest to establish and manipulate long-range quantum networks. In the context of a three-qubit state, it may possess bipartite or a tripartite nonlocality. If one wishes to utilize the properties of genuine three-qubit nonlocality, one must be able to identify states with genuine three-qubit quantum correlations. As against the original Mermin and Svetlichny inequalities, our inequalities using cluster coefficients not only distinguish between bipartite and tripartite nonlocalities, but are also violated by all pure three-qubit genuinely

entangled states. In order to understand the intricacies involved and to perform a comparative study, we also extended our analysis to noisy channels and described nonlocal properties in different sets of three-qubit entangled and mixed states. Table 3.1 summarizes the results obtained in this chapter for various three-qubit pure and mixed states. In comparison to the modified

Table 3.1 : Summary of three-qubit nonlocality operators for various three qubit states

S.No.	State	Mermin	Svetlichny	$\text{Mermin}_{\text{cum}}$	$\text{Svetlichny}_{\text{cum}}$
	Classical bound	2	4	0	0
1)	$\|\psi_A\rangle \otimes \|\psi_B\rangle \otimes \|\psi_C\rangle$	2	4	0	0
2)	$\|\phi^+\rangle_{AB} \otimes \|\psi_C\rangle$	4	0	0	
3)	$\|GHZ\rangle$	4	$4\sqrt{2}$	4	$4\sqrt{2}$
4)	$\|\psi_{GHZ}\rangle$	2 to 4*	4 to $4\sqrt{2}$**	0 to 4	0 to $4\sqrt{2}$
5)	$\|\Phi\rangle$	$2\sqrt{2}$ to 4	4 to $4\sqrt{2}$	0 to 4	0 to $4\sqrt{2}$
6)	$\|\psi_{MS}\rangle$	$2\sqrt{2}$ to 4	4 to $4\sqrt{2}$	0 to 0 to $4\sqrt{2}$	0 to $4\sqrt{2}$
7)	$\|W\rangle$	3.0460	4.3546	1.9397	2.7541
8)	$\|\psi_W\rangle$	$2\sqrt{2}$ to 3.046	4 to 4.3546	0 to 1.9397	0 to 2.7541
9)	$\|W_n\rangle^\dagger$	3 to 2.8819	4.2762 to 4.0854	1.7321 to 0.8347	2.4495 to 1.1807
10)	$\|W_1\rangle$	3	4.2762	1.7321	2.4495
11)	ρ_a	0 to 4	0 to $4\sqrt{2}$	0 to 4	0 to $4\sqrt{2}$
12)	ρ_b	0 to 3.046	0 to 4.3546	0 to 1.9397	0 to 2.7541
13)	ρ_c	3.046 to 4	4.3546 to $4\sqrt{2}$	1.8452 to 4	2.6978 to $4\sqrt{2}$

* violation for $\theta > \frac{\pi}{12}$; ** violation for $\theta > \frac{\pi}{8}$; † $n \in [1, 11]$.

Svetlichny operator, the evaluation of nonlocality using modified Mermin operator is relatively less complicated because of the less number of expectations values involved in the expression of the Mermin operator. Nevertheless, the nonlocal properties using both operators for all states lead to similar observations with a larger violation of the modified Svetlichny inequality in comparison to the modified Mermin inequality.

Increasing one more qubit to three qubit states results in increased number of classes withing the sets of pure four qubit states. In addition to the genuine four-qubit nonlocality, one would also need to worry about tripartite and bipartite nonlocality. Furthermore, there exist different inequalities for different classes of pure states and many of these inequalities further fail to identify genuine nonlocality in multi-qubit states. In the next chapter, we take our discussion forward to the case of four and five qubit states.

...